



Tutorial and simulations with ADAM: an adaptation and anticipation model of sensorimotor synchronization

Bronson Harry¹ · Peter E. Keller¹

Received: 27 July 2018 / Accepted: 1 April 2019 / Published online: 8 April 2019
© Springer-Verlag GmbH Germany, part of Springer Nature 2019

Abstract

Interpersonal coordination of movements often involves precise synchronization of action timing, particularly in expert domains such as ensemble music performance. According to the adaptation and anticipation model (ADAM) of sensorimotor synchronization, precise yet flexible interpersonal coordination is supported by reactive error correction mechanisms and anticipatory mechanisms that exploit systematic patterns in stimulus timing to plan future actions. Here, we provide a tutorial introduction to the computational architecture of ADAM and present a series of single- and dual-virtual agent simulations that examine the model parameters that produce ideal synchronization performance in different tempo conditions. In the single-agent simulations, a virtual agent synchronized responses to steady tempo sequence or a sequence containing gradual tempo changes. Parameters controlling basic reactive error (phase) correction were sufficient for producing ideal synchronization performance at the steady tempo, whereas parameters controlling anticipatory mechanisms were necessary for ideal performance with a tempo-changing sequence. In the dual-agent simulations, two interacting virtual agents produced temporal sequences from either congruent or incongruent internal performance templates specifying a steady tempo or tempo changes. Ideal performance was achieved with reactive error correction alone when both agents implemented the same performance template (either steady tempo or tempo change). In contrast, anticipatory mechanisms played a key role when one agent implemented a steady tempo template and the other agent implemented a tempo change template. These findings have implications for understanding the interplay between reactive and anticipatory mechanisms when agents possess compatible versus incompatible representations of task goals during human–human and human–machine interaction.

Keywords Sensorimotor synchronization · Interpersonal coordination · Cognitive modeling · Action timing · Temporal prediction

1 Introduction

The capacity to coordinate bodily movements in time with external events is fundamental to human social behavior. Many forms of cooperative interaction involve interpersonal coordination of actions across two or more individuals. Although action synchronization can occur spontaneously (e.g., during applause, (Néda et al. 2000)), interactions that call for precise yet flexible movement timing between

individuals, such as musical ensemble performance, typically involve intentional goal-directed motor planning and control (Keller 2008; Keller et al. 2014; Sebanz and Knoblich 2009).

The mechanisms that support real-time interpersonal coordination have been studied in the laboratory using basic sensorimotor synchronization tasks whereby individuals perform simple movements (i.e., finger tapping or drumming) in time with rhythmic auditory-pacing stimuli produced by a computer or another person (Konvalinka et al. 2010; Nowicki et al. 2013; Pecenka and Keller 2011; Repp 2005; Repp and Su 2013). Computational models designed to elucidate the underlying causes of behavioral phenomena observed in sensorimotor synchronization tasks can be broadly classified as either nonlinear dynamic models or linear event-based models. Both varieties of model have been used to drive virtual partners that provide potential

Communicated by Benjamin Lindner.

✉ Bronson Harry
b.harry@westernsydney.edu.au

¹ Music, Cognition and Action Group, The MARCS Institute for Brain, Behaviour and Development, Western Sydney University, Locked Bag 1797, Penrith, NSW 2751, Australia

platforms for applications requiring precise human–machine interaction (Dumas et al. 2014; Fairhurst et al. 2013, 2014; Kelso et al. 2009; Mills et al. 2015; Repp and Keller 2008).

Nonlinear dynamic models account for continuous cyclic aspects of sensorimotor synchronization behavior in terms of coupled oscillators that interact in such a way that activity in the motor system becomes synchronized with external rhythmic stimuli (Dumas et al. 2014; Large et al. 2015; Loehr et al. 2011; McAuley and Jones 2003; Tognoli and Kelso 2014). In contrast, linear event-based models take a discrete information processing approach to specifying time points for upcoming actions by applying autoregressive procedures that adjust an internal timekeeper based on the timing of past actions and perceptual events (Hary and Moore 1987; Jacoby and Repp 2012; Mates 1994a; Michon 1967; Pressing 1999; Schulze et al. 2005; van der Steen and Keller 2013; Vorberg and Wing 1996). These classes of models are not mutually exclusive, and efforts to reconcile these two modeling approaches range from formal unification wherein both linear and nonlinear behavioral features are accommodated (Bavassi et al. 2013); to views that they are complementary and deal with different aspects of sensorimotor synchronization: the continuous within-cycle dynamics of movement trajectories versus between-cycle information about time intervals marked by sequential event onsets (MacRitchie et al. 2017; Torre and Balasubramaniam 2009; van der Steen and Keller 2013).

The present article is concerned with modeling discrete goal-directed cases of sensorimotor synchronization using the linear event-based approach. Specifically, we present a tutorial overview of the recently developed adaptation and anticipation model (ADAM) of sensorimotor synchronization (Keller et al. 2016; van der Steen et al. 2015; van der Steen and Keller 2013). According to ADAM, interpersonal synchronization is established and maintained by two main

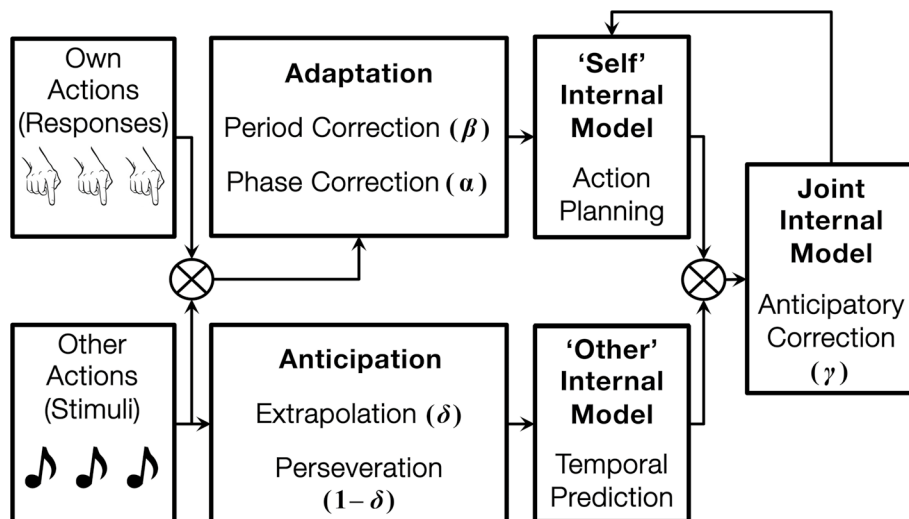
classes of control process—temporal adaptation and anticipation—that are implemented as separate modules (Fig. 1). The adaptation module includes reactive error correction mechanisms that adjust planned actions based on recent synchronization errors, while the anticipation module includes predictive processes that estimate the likely timing of future stimulus events. A third ‘joint’ module links the adaptation and anticipation modules by implementing anticipatory error correction to reduce potential discrepancies between plans and predictions prior to action execution.

The aim of the present study is to provide a simple introduction to ADAM and to demonstrate how this model can be applied to simulate phenomena observed in real-world interpersonal synchronization. In the following, we first provide a conceptual review and formal description of computational processes instantiated by the adaptive, anticipatory, and joint modules of the model. We then provide a series of simulation studies designed to: (1) illustrate how parameters in ADAM’s modules behave under conditions of unidirectional coupling with pacing sequences presented at a constant tempo or with varying tempo (as in standard laboratory experiments) and (2) demonstrate how ADAM can be used to explore more complex forms of bi-directional coupling arising during interpersonal synchronization (e.g., musical duos).

2 Discrete event framework and model architecture

The three modules of ADAM work together to control movement timing based on information related to stimulus onsets (other actions, e.g., pacing tones), response onsets (own actions, e.g., finger taps), and parameter settings representing latent sensory-motor and cognitive processes. The

Fig. 1 Schematic diagram of the adaptation and anticipation model (ADAM). The synchronization of one’s own actions (responses) with another’s actions (stimuli) is facilitated by temporal adaptation mechanisms that influence action planning, anticipation mechanisms that enable temporal prediction, and an anticipatory correction mechanism that reduces discrepancies between plans and predictions



main components of ADAM are illustrated in Fig. 2 and the equations describing its operations are listed in Table 1. In this context, stimulus onsets S_i and response onsets R_i refer to the time since the start of the experimental trial (Fig. 2a). By extension from conventional approaches to sensorimotor synchronization, responses produced by each agent serve as the stimulus to their respective partner. Inter-stimulus onset and inter-response onsets are denoted as s_i and r_i , given by Eqs. (1) and (2) in Table 1. Asynchronies between stimuli and responses, denoted by A_i , are given by Eq. (3), such that negative asynchronies occur when responses precede stimulus onsets.

2.1 Adaptation

The temporal adaptation mechanisms implemented in ADAM are inherited from linear autoregressive models of SMS. Core components of these models are a central timekeeper, a motor implementation process that executes responses, and error correction mechanisms that influence the timekeeper and motor implementation (Hary and Moore

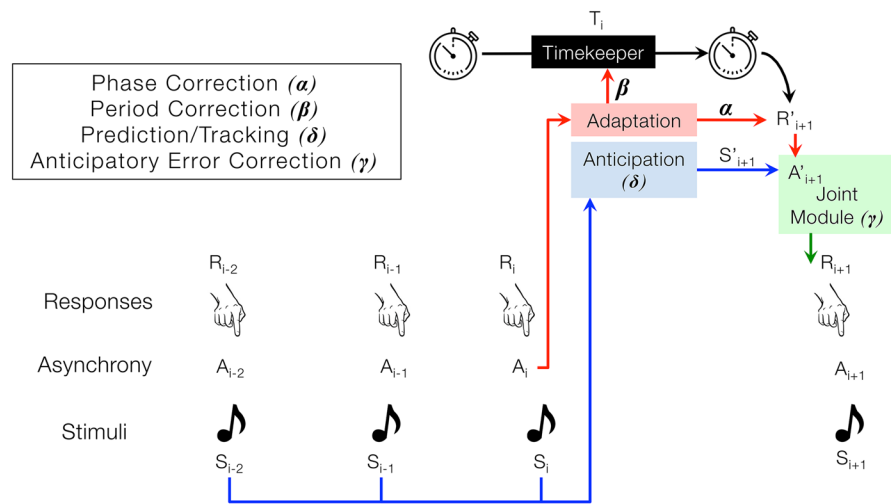
Table 1 Equations describing the event-related framework (1–3) and the operations implemented by the three modules of ADAM (4–10)

$s_i = S_i - S_{i-1}$	(1)
$r_i = R_i - R_{i-1}$	(2)
$A_i = R_i - S_i$	(3)
<i>Adaptation module</i>	
$R'_{i+1} = R_i + T_i - \alpha \times A_i + nT_i$	(4)
$T_i = T_{i-1} - \beta \times A_i$	(5)
<i>Anticipation module</i>	
$S'_{i+1} = S_i + \delta \times e_{i+1} + (1 - \delta) \times p_{i+1} + nT_i$	(6)
$e_{i+1} = 2 \times s_i - s_{i-1}$	(7)
$p_{i+1} = s_i$	(8)
<i>Joint module</i>	
$A'_{i+1} = R'_{i+1} - S'_{i+1}$	(9)
$R_{i+1} = R'_{i+1} - \gamma \times A'_{i+1} + nM_{i+1} - nM_i$	(10)

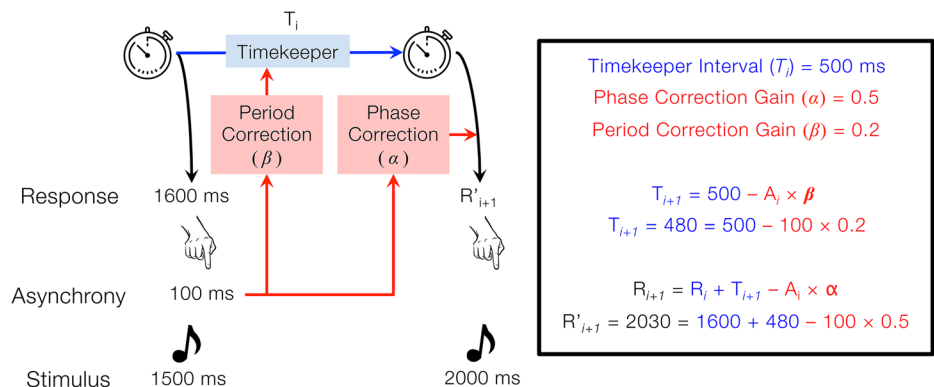
S , stimulus onset; R , response onset; s , stimulus interval, r , response interval, A , asynchrony, T , timekeeper interval; R' , planned response onset; S' predicted stimulus onset; A' , anticipated error; e , extrapolated stimulus interval; p , perseverated stimulus interval; nT , timekeeper noise; nM , motor noise; α , phase correction, β , period correction; δ , prediction/tracking weight; γ , anticipatory error correction

Fig. 2 Main components of the ADAM framework. **a** Relationship between stimuli (S_i), responses (R_i), and the asynchrony between stimuli and responses (A_i). ADAM expresses the timing of actions (R_{i+1}) in terms of previous stimuli, responses, an internal timekeeper and compensatory mechanisms comprising the adaptation, anticipation and joint modules. **b** Depicts a simplified (noise terms omitted) example of reactive error correction. In this example, the auditory stimulus sequence comprises isochronous intervals of 500 ms. The timekeeper is assumed to have accurately stored the interval of the sequence; however, an asynchrony is observed in the first interval such that the response was produced 100 ms after the stimulus. Period correction is applied with a gain of 0.2, which reduces the interval stored in the timekeeper by 20 ms. Phase correction is applied with a gain of 0.5, which adjusts the upcoming response by half of the most recent asynchrony (50 ms)

(a) Adaptation & Anticipation Model



(b) Adaptation Module



1987; Jacoby and Repp 2012; Mates 1994a; Michon 1967; Pressing 1999; Schulze et al. 2005; van der Steen and Keller 2013; Vorberg and Schulze 2002; Vorberg and Wing 1996).

It is assumed that the central timekeeper has access to a memory representation of the period defined by inter-onset intervals in the pacing stimulus and uses this representation as a basis for controlling the rate at which motor commands are issued during SMS. Error correction mechanisms serve to adjust the timing of action execution to minimize asynchronies and prevent tempo drift between sequential actions and stimuli. These correction mechanisms compensate for sources of variability that arise both in the central and peripheral nervous system (Vorberg and Hambuch 1978; Wing 1993; Wing and Kristofferson 1973), termed timekeeper noise and motor noise, respectively. Timekeeper noise is assumed to scale with the size of the interval stored in memory and increases with the magnitude of the timekeeper interval (though relatively high variability is also observed for very short intervals; i.e., < 300 ms; Repp 2005). Motor noise, which arises during transmission of signals to the effectors and varies as a function of nerve conduction time and biomechanical constraints, is assumed to be independent of the duration of the interval being produced (Vorberg and Wing 1996; Wing and Kristofferson 1973). Estimates of motor noise are typically smaller than estimates of timekeeper noise in self-paced timing tasks (Wing and Kristofferson 1973), as well as in sensorimotor synchronization tasks (van der Steen et al. 2015), and introducing the constraint that motor variance does not exceed timekeeper variance produces optimal solutions in computational modeling of sensorimotor synchronization (Jacoby et al. 2015).

Error correction mechanisms proposed in linear models are *reactive* in the sense that asynchronies between past actions and events trigger compensatory adjustments to future motor plans. A conceptual distinction has been drawn between two types of error correction process; phase correction, which locally adjusts the phase relationship between actions and stimulus events, and period correction, which directly adjusts the timekeeper period, bringing about a persistent, global change to the rate that motor commands are issued by the timekeeper (Mates 1994a, b). Formally, the difference between phase correction and period correction is that, while phase correction directly influences the next planned response time, period correction indirectly influences the next response by changing the underlying timekeeper period. Moreover, whereas phase correction is assumed to be automatic, period correction requires attention and awareness of a change in tempo (Repp and Keller 2004). However, although phase correction is automatic, its gain can be modulated based on task demands. Phase correction increases as tempo decreases and synchronization becomes more challenging (Repp et al. 2012). Furthermore, the results of simulations with virtual partners that vary in

cooperativity (i.e., amount of error correction) have revealed that, while human phase correction remains constant across a range of cooperative partners, its gain can be increased when confronted with uncooperative partners (Fairhurst et al. 2014; Repp and Keller 2008).

In ADAM's adaptation module, the central timekeeper (T) controls the timing of motor commands that trigger movements during sensorimotor synchronization, and phase (α) and period (β) correction modify the timing of the next movement based on a proportion of the asynchrony between the previous movement and its synchronization target. The phase correction parameter (α) in ADAM represents the proportion of each asynchrony (A_i) that is automatically corrected for in the next response and thus indexes the strength of sensorimotor coupling or entrainment (see Fig. 2b for an example). The effect of phase correction on the output of the adaptation module (R'_{i+1}) is expressed in Eq. (4) in Table 1, where R_i is the time at which the most recent movement occurred, T_i is the current timekeeper interval used to plan the next response, α is the phase correction parameter, A_i is the most recent asynchrony between response and stimulus and R'_{i+1} is the planned time of the next response.

The period correction parameter (β) directly adjusts the period of the timekeeper and represents the proportion of each asynchrony (A_i) that is corrected in the next response based on conscious detection of a synchronization error. The effect of period correction on the timekeeper interval (T) is expressed in Eq. (5), where T_i is the most current timekeeper interval and nT_i represents a noise term associated with the timekeeper (which is modeled by drawing a value from a normal distribution).

2.2 Anticipation

ADAM's anticipation module estimates the timing of upcoming sounds in an external pacing sequence by weighting processes of extrapolation versus perseveration of earlier inter-onset intervals in the sequence. The development of this module was motivated by the results of finger-tapping studies using expressive musical performances or simple tone sequences containing gradual tempo changes resembling those found in such performances (Pecenka and Keller 2009, 2011; Rankin et al. 2009; Repp 2002; Schulze et al. 2005). These studies revealed variations in the degree to which inter-response intervals match versus lag behind pacing inter-stimulus intervals across experimental conditions and individuals. Notably, the tendency to predict tempo changes is positively correlated with musical experience, and these individual differences are related to the accuracy and stability of synchronization with computer controlled pacing sequences and sounds produced by another individual during dyadic finger tapping (Pecenka and Keller 2011). Temporal anticipation appears to rely on relatively high-level

cognitive processes, as tempo change prediction is impaired under conditions of increased attention load (Pecenka et al. 2013) and individual differences are positively correlated with working memory capacity (Colley et al. 2017) and auditory imagery ability (Pecenka and Keller 2009).

Formally, in ADAM (van der Steen et al. 2015a; van der Steen and Keller 2013), the anticipation module generates prospective estimates of the timing of the next event (S'_{i+1}) in a pacing sequence based on the weighted sum of extrapolation and perseveration processes. The active extrapolation process (e_{i+1}), which is assumed to be effortful, entails linear extrapolation of the two most recent inter-stimulus intervals (s_i and s_{i-1}). The automatic perseveration (p_{i+1}) process copies the current inter-onset interval (s_i). The balance of prediction and tracking are controlled by the weighting parameter δ . The anticipated timing of the next pacing event (S'_{i+1}) is expressed in Eq. (6) in Table 1, where the anticipated inter-onset interval is based on a weighted sum of two estimates of the future inter-stimulus interval. The first estimate is based on extrapolation (e_{i+1}) and is determined by linear extrapolation according to Eq. (7), and the second estimate is based on perseveration (p_{i+1}) the previous inter-stimulus onset (8). The anticipated timing of the next pacing event is determined entirely through tempo extrapolation when $\delta=1$ and entirely through tracking when $\delta=0$. Similar to the adaptation module, the predicted stimulus onset is also affected by timekeeper noise. Here, we assume that both modules are affected by the same noise source (nT_i).

2.3 Links between adaptation and anticipation

While temporal adaptation and anticipation have traditionally been studied separately, there is empirical evidence that they are linked. A study assessing adaptation and anticipation in the same sample of individuals found that estimates of phase correction and temporal prediction are positively correlated, and that these adaptive and anticipatory processes in combination explain a large amount of variance in sensorimotor synchronization skill (Mills et al. 2015). ADAM accounts for these links in a joint module that regulates the balance between the output of the adaptation and anticipation modules.

Conceptually, it is assumed that the adaptation module initially provides input to a ‘self’ internal model that plans the timing of one’s own next action, while the anticipation module provides input to an ‘other’ internal model that generates a prediction about the timing of the next sound in the pacing sequence. In general, internal models represent sensorimotor associations between motor commands that issue from the brain and the sensory experience of events in the environment,

allowing actions to be simulated in the motor system independently of their actual execution (Wolpert and Kawato 1998). It has been proposed that internal models thus facilitate the planning and online control of one’s own actions, as well as the prediction of others’ actions during social interaction (Blakemore and Frith 2005; Gambi and Pickering 2011; Keller 2008; Knoblich and Jordan 2003; Sanger et al. 2011; Wolpert et al. 2003). ADAM’s joint module integrates these processes by computing the discrepancy between outputs of the ‘self’ and ‘other’ internal models and then adjusts the ‘self’ model to compensate for this discrepancy before a motor command is issued (Keller et al. 2016). Joint internal models thus facilitate interpersonal coordination by allowing potential asynchronies between ‘own’ action plans and ‘other’ predicted actions to be corrected in advance.

Formally, ADAM’s joint module takes the outputs of the adaptation and anticipation modules and computes the expected asynchrony (A'_{i+1}) between them, as shown in Eq. (9) in Table 1. An anticipatory error correction process (γ) then compensates for a proportion of this discrepancy, and the timing of the next movement (R_{i+1}) is determined by modifying the output of the adaptation module (R'_{i+1}) according to Eq. (10). When $\gamma=0$, movement timing is determined entirely by the output of the adaptation module and is formally identical to traditional reactive error correction models (Jacoby and Repp 2012; Schulze et al. 2005; Vorberg and Wing 1996). When $\gamma=1$, movement timing is determined entirely by the output of the anticipation module.

In ADAM (as in the linear event-based models from which it evolved) it is assumed that, once a motor command issues from the central nervous system, the timing of the actual movement is affected by ‘motor’ noise (nM_i , nM_{i+1}) in the peripheral nervous system. Motor noise introduces a random variable delay, which can be modeled by drawing a value from a Gamma distribution. Also, the noise associated with the most recent transmission delay (nM_i) is subtracted from the most recent response onset. This equation captures the alternating pattern of short and long inter-response intervals (negative lag-1 autocorrelation) observed in continuation tapping tasks where participants tap at a steady tempo without a pacing stimulus (Wing and Kristofferson 1973). Under this scheme, motor plans are issued centrally based on information from timekeeper and compensatory mechanisms (adaptation, anticipation) that do not take into account the previous delay caused by peripheral noise (Vorberg and Wing 1996). Note that we discuss motor noise here only to provide a full account of the ADAM. For the sake of simplicity, motor noise was not included in the simulations because it is typically small and relatively constant in magnitude (see Wing et al. 2014 for a similar approach).

3 Model simulations

To illustrate the key properties of the model, we carried out a series of computer simulations that highlight how ADAM's adaptation, anticipation, and joint modules influence sensorimotor synchronization in different task contexts. Van der Steen et al. (2015a, b) extended classical work by presenting an analysis of the properties of autoregressive models incorporating anticipatory mechanisms. The focus of that study was to assess which of two different computational architectures for integrating adaptive and anticipatory mechanisms was the best fit to sensorimotor synchronization data collected from various tempo-changing tasks. In these tasks, participants synchronized finger taps to auditory-pacing sequences wherein the inter-stimulus interval predictably increased and decreased. The primary finding was that models incorporating a joint module provided a better fit to tempo change data than so-called hybrid models that did not.

Although van der Steen et al. (2015a, b) carried out multiple simulations to support the main findings of their study, a full characterization of the model—particularly the role of anticipatory error correction—has yet to be presented. To help simplify the simulations presented in van der Steen et al. (2015a, b), the value assigned to anticipatory error correction parameter was always set to a fixed value, and parameters from the adaptation and anticipation modules were varied. So it remains to be seen how anticipatory error correction interacts with adaptive and anticipatory mechanisms to affect sensorimotor synchronization performance. Moreover, the simulations in van der Steen et al. (2015a, b) were only carried out on tempo-changing stimulus sequences, raising the question about what role the anticipation and joint modules play for more traditionally studied isochronous sequences that do not contain any changes in tempo.

Accordingly, the aim of the present study was to provide a full simulation-based analysis of the ADAM across a range of conditions. Specifically, the simulations aimed to identify the parameters that were necessary and sufficient for producing optimal sensorimotor synchronization according to two commonly assessed criteria: (1) accuracy, indexed inversely by the mean asynchrony, which quantifies the average magnitude of the synchronization error during a trial and (2) variability, indexed by the standard deviation of the asynchronies, which (inversely) quantifies the stability of synchronization errors during a trial. Our main focus is on achieving stability because mean asynchrony may vary as a function of factors including leader–follower relations and stylistic features such as groove (Keller et al. 2014).

The optimal parameter settings were assessed under two task contexts—steady tempo and tempo change—that

correspond to different real-life scenarios that vary in terms of demands related to temporal adaptation and anticipation. Maintaining a steady tempo while coordinating with others—at least for some portion of the activity—is a common goal in ensemble music, dance, and some team sports (e.g., rowing). In these cases, adaptation is necessary to counteract natural variations in timing due to noise in the motor system as well as unforeseen circumstances that perturb coordination. In contrast, anticipation demands should be low to the extent that predicting future stimulus onsets can be based on the assumption that future synchronization targets arrive at a regular interval.

Demands associated with coordination in the context of tempo changes are relatively high. Intentional tempo variations occur in musical ensemble performance to highlight musical structural features and to signal emotional emphasis and fluctuations in arousal and tension (Gabrielsson 2003; Keller et al. 2016). Likewise, tempo variations can be observed in sporting activities, such as when a rowing crew initially accelerates at the start of a race (Edwards et al. 2016). Under such circumstances, temporal anticipation entails estimating the onset of future synchronization targets from the rate of change observed in previous events, and thus may require effortful forms of prediction.

Steady tempo and tempo change scenarios were explored under two conditions: single-agent and dual-agent, presented here as separate sets of simulations. The single-agent simulations address instances of human–machine synchronization where the machine-controlled sequences are not influenced by the human's timing. The dual-agent simulations represent instances of human–human synchronization where both agents can mutually adapt to one another. The goal of the single-agent simulations was to evaluate each model parameter in isolation, in a simplified interaction where only a single agent could adapt to or anticipate the other's timing. The goal of the dual-agent simulations was to examine each model parameter in a more complex, naturalistic interaction where each agent could adapt to and/or anticipate the other's timing.

Finally, we also calculated two measures that capture time-varying aspects of performance that are commonly reported in sensorimotor synchronization experiments. The first measure was the lag-1 autocorrelation of the asynchronies (Vorberg and Schulze 2002; Wing et al. 2014), which is influenced by error correction and can hence provide an indirect, data-driven estimate of the overall effects of correction-related behavior implemented by the model. When positive, the lag-1 autocorrelation of the asynchronies indicates that the system is not fully correcting timing errors whereas when negative, this measure indicates that the system is overcompensating for timing errors.

The second measure, based on lag-1 and lag-0 cross-correlations of inter-response intervals and inter-stimulus

intervals (for single-agent simulations) or the inter-response intervals of two agents (in dual-agent simulations), is used to quantify how well the sequence of response intervals for an agent matches the sequence of stimulus intervals (single-agent) or the sequence of response intervals of a simulated partner (dual-agent). A high lag-0 correlation indicates that the pattern of inter-response intervals and reference intervals (inter-stimulus intervals for single-agent and the partner’s inter-response intervals for dual-agent) were well matched, suggesting that the upcoming reference interval could be predicted. In contrast, a high lag-1 value indicates that the inter-response intervals tended to lag behind the reference intervals, indicative of tracking behavior. These cross-correlations can be combined to provide a data-driven measure of how well the reference intervals are predicted in tempo-changing tasks (e.g., Pecenka et al. 2013; Repp 2002; van der Steen et al. 2015a) or to assign leader–follower status for mutually coupled agents (e.g., Konvalinka et al. 2010).

The MATLAB code used for all simulations presented in this paper is available for download from the Open Science Framework (available at: <https://osf.io/nc3zw/>).

4 Single-agent simulations

Based on previous work combining behavioral sensorimotor synchronization experiments with computer simulations (e.g., Repp and Keller 2008), we expected that the phase correction parameter (α) from ADAM’s adaptation module would be necessary and sufficient for maximizing the stability of synchronization in the steady tempo simulations. In line with previous work, the optimal value of the phase correction parameter was expected to be $\alpha = 1$ (Vorberg 2005; Wing et al. 2014). Once phase correction (α) is optimized, adding other parameters—period correction (β) in the adaptation module and the prediction/tracking weight (δ) in the anticipation module—should not lead to further improvement, because these parameters control mechanisms that are necessary to deal with tempo variations. Specifically, changes to timekeeper interval via period correction (β) are useful only when the stimulus inter-onset interval undergoes systematic change. Furthermore, varying the prediction/tracking weight (δ) was not expected to have an effect on synchronization performance because extrapolation ($\delta = 1$) and tracking ($\delta = 0$) parameter settings produce the same predicted stimulus onset (S'_{i+1}) for isochronous sequences. It was unclear whether anticipatory error correction implemented in the joint module would improve performance once phase correction was optimized. When optimized, phase correction fully compensates for the most recent asynchrony (A_i) in the timing of the next planned response (R_{i+1}). In this situation, the only error that cannot be accounted for by phase correction is the noise from the timekeeper in the planned response (nT_i). However, timekeeper noise also

affects the anticipated stimulus onset time produced by the anticipation module. Thus, the planned response onset and the anticipated stimulus onset would be equal, producing no anticipated error for the joint module to correct. If true, then anticipatory error correction would only improve performance when phase correction is suboptimal.

For the case of synchronizing with tempo-changing sequences, it was expected that optimizing phase correction (α) would be necessary but not sufficient for maximizing precision. In other words, after optimizing phase correction (α), the addition of period correction (β), prediction/tracking weighting (δ), and anticipatory error correction (γ) capacities should lead to improvement. Since accurately predicting future intervals in tempo-changing sequences relies on extrapolating the rate of tempo acceleration or deceleration from previous events, it was expected that prediction/tracking weighting and anticipatory error correction would play a critical role in producing ideal performance. However, given that predictions can overshoot actual events at reversal points in tempo change profiles (van der Steen et al. 2015a), the specific settings for these additional parameters constitute an open question.

4.1 Procedure

Simulations were carried out with custom scripts running in MATLAB 2014b. The stimulus sequence for the steady tempo condition comprised 68 isochronous intervals of 500 ms (Fig. 3, as in a typical sensorimotor synchronization experiment; see Repp 2005; Repp and Su 2013). The second ‘tempo change’ sequence comprised four initial isochronous intervals presented at 500 ms, followed by 64 non-isochronous intervals that varied predictably from 400 to 600 ms, with an average inter-stimulus interval of 500 ms (similar to Mills et al. 2015; Pecenka and Keller 2011; van der Steen et al. 2015a). The rate of tempo change for these sequences was determined with the function found in Eq. (11)

$$s_i = 500 + 100 \times \cos \left(\frac{(i - 4) \times \pi}{8} \right). \tag{11}$$

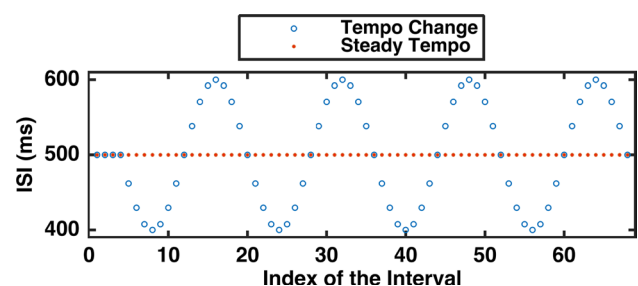


Fig. 3 Inter-stimulus intervals for the tempo change condition (blue) and the steady tempo condition (red) (color figure online)

Parameter selection involved a grid search technique whereby mean signed asynchrony and standard deviation of asynchrony was calculated for each combination of selected parameter settings. For the steady tempo condition, phase correction (α) and period correction (β) in the adaptation module were selected from the range 0–2 at an interval of 0.05. The prediction/tracking weight (δ) in the anticipation module was set to 0 (i.e., full tracking) in this condition since both prediction (extrapolation) and tracking (perseveration) produce identical estimates for the anticipated stimulus onset (S'_{i+1}) for isochronous sequences. Anticipatory error correction (γ) values in the joint module were selected from the range 0–1 at an interval of 0.1 for the steady tempo simulations. Note that the ‘planned’ timing of the next response is determined entirely on the output of the adaptation module when $\gamma=0$. For the tempo change condition, simulations were run for phase (α) and period correction (β) values ranging between 0 and 2 with 0.05 intervals, prediction/tracking weight (δ) between 0 and 1 with 0.5 intervals, and anticipatory error correction (γ) between 0 and 1 with 0.1 intervals.

A total of 1000 simulations were run for each combination of parameters for each of the two stimulus sequences. The initial timekeeper interval was set to match the average pacing sequence interval for each simulation trial ($T_1=500$ ms). Timekeeper noise was simulated by drawing a single random value from a normal distribution with a mean of zero and standard deviation of 10 and adding this value to the output of the adaptation (R'_{i+1}) and anticipatory modules (S'_{i+1}). A new random value was sampled for each interval in the stimulus sequence. The seed used to initialize the random number generator responsible for producing timekeeper noise was identical for each parameter combination examined by the grid search technique. Mean signed asynchrony (indexing synchronization accuracy), mean absolute asynchrony, and the standard deviation of asynchronies (synchronization stability) were calculated for each simulation and then averaged over the 1000 simulations for each parameter combination. While we were primarily concerned with synchronization stability, synchronization accuracy was assessed to establish whether, for a given set of parameters, the model was synchronizing in an in-phase relationship.

In addition, the lag-1 autocorrelation of asynchronies and the lag-1 and lag-0 ISI–IRI cross-correlations were calculated for each simulation and averaged in the same manner as the other performance measures. For the tempo-changing condition, the lag-0 and lag-1 cross-correlations yield similar values that do not readily reveal the differences between these two measures. Thus, to emphasize the differences between these two values, the prediction/tracking ratio (PTR; Pecenka et al. 2013; van der Steen et al. 2015a) was calculated as the ratio of the lag-0 and the lag-1 of the ISI–IRI cross-correlations, where a prediction/

tracking ratio less than 1 indicates that IRIs lagged behind the ISIs by one interval (i.e., indicative of tracking responses), and a prediction/tracking ratio greater than 1 indicates that IRIs were a better match to current ISIs than to interval-lagged ISIs.

4.2 Results

4.2.1 Steady tempo

Mean signed asynchrony ranged from -0.2 ms to extremely high values (due to exponential growth in asynchronies with poor parameter settings). The mean signed asynchrony was practically identical for all parameter settings that produced stable performance (as defined by the standard deviation of asynchronies below) and will not be considered further. The mean absolute asynchrony and the standard deviation of asynchronies ranged from 7.97 and 9.94 ms upwards across the various ADAM parameter settings for simulated synchronization with the steady tempo sequence. Specific parameter settings produced generally similar patterns of results on mean absolute asynchrony and the standard deviation of asynchronies, so only data for the standard deviation of asynchronies are presented below (see Fig. 4a–c). Anticipatory error correction had a monotonic effect on synchronization performance, and so performance is only shown across three anticipatory error correction settings (Fig. 4a, $\gamma=0$; 4b, $\gamma=0.5$; 4c, $\gamma=1$). Each plot shows the standard deviation of asynchronies—inversely indexing synchronization stability—as a function of phase correction (x -axis) and period correction (y -axis).

Considering first simulations with no anticipatory error correction ($\gamma=0$; Fig. 4a, left panel), ideal performance in terms of synchronization stability was observed when full phase correction ($\alpha=1$) and no period correction were applied. The standard deviation of asynchronies reached a minimum of 9.94 ms with these parameter settings (mean signed asynchrony for this parameter setting was 0.4 ms). This value is essentially equal to timekeeper variability (10 ms), indicating that optimal phase correction completely compensated for the timing error associated with the previous interval. Parameter settings incorporating only period correction produced unstable performance resulting from large asynchronies that increased over the course of the trial (Fig. 4e). Likewise, very high levels of reactive error correction (overall sum of phase and period correction, Fig. 4f) produced unstable performance. Thus, only phase correction is required to produce ideal performance.

Considering now the effect of anticipatory error correction, as this parameter increases (Fig. 4a–c), stable performance was observed across a greater range of phase and period correction settings, indicating a reduced need for reactive error correction with increased use of anticipatory

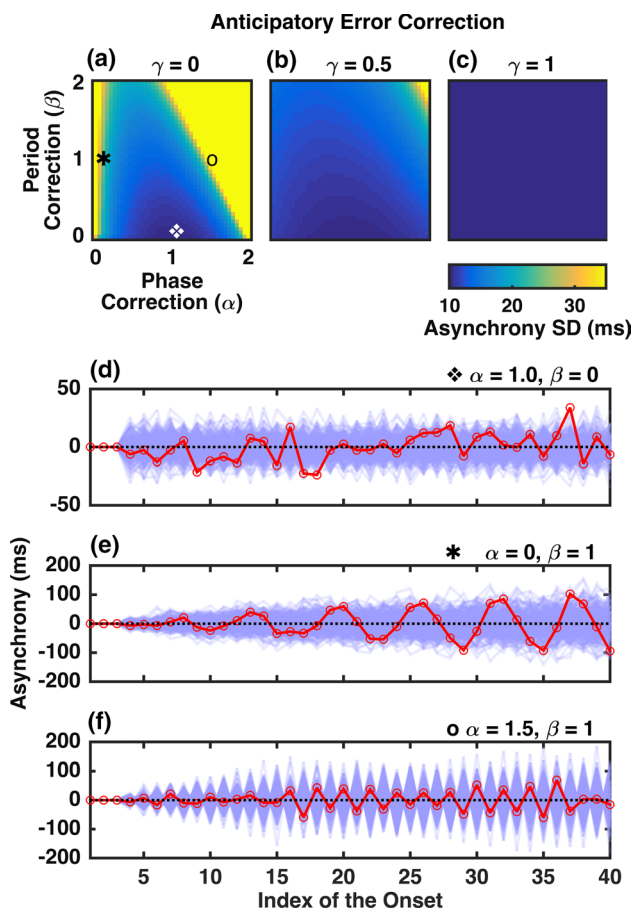


Fig. 4 Effect of ADAM parameters on single-agent sensorimotor synchronization in the steady tempo condition. **a–c** Standard deviation of asynchronies observed for the steady tempo condition as a function of phase correction (*x*-axis), period correction (*y*-axis) and anticipatory error correction (separate panels). Panels depict performance across different levels of anticipatory error correction (**a**, $\gamma = 0$; **b**, $\gamma = 0.5$; **c**, $\gamma = 1$). **d–f** Asynchrony timecourse plots for different example parameter settings for 250 simulations (purple) and one representative trial (red). **d** Optimal parameter setting ($\alpha = 1$). An identical asynchrony timecourse is produced for full anticipatory error correction ($\gamma = 1$). Unstable parameter settings produced with full period correction (**e**, $\alpha = 0, \beta = 1$) and overcorrection (**f**, $\alpha = 1.5, \beta = 1$). Note the larger scale of the *y*-axis in plots **e–f** compared to **d** (color figure online)

error correction. Indeed, with full anticipatory error correction, reactive error correction no longer affected performance (indicated by the uniform color in the right panel). The minimum standard deviation of asynchronies for simulations applying full anticipatory error correction ($\gamma = 1$) was identical to the minimum standard deviation of asynchronies observed with full phase correction ($\alpha = 1$) and no anticipatory error correction ($\gamma = 0$). It can also be noted that simulations applying full anticipatory error correction produced identical stimulus and response onsets (and consequently asynchronies) as simulations that applied no anticipatory error correction and full phase correction (see Fig. 4b). This correspondence suggests that—at least in the case of

isochronous sequences—full anticipatory error correction in ADAM’s joint module is functionally equivalent to full phase correction in the adaptation module.

Taken together, the results of the present set of simulations suggest that, in ADAM’s adaptation module, phase correction (α) is both necessary and sufficient to account for stable sensorimotor synchronization performance, whereas period correction (β) generally has a deleterious effect under steady tempo conditions. By definition, the prediction/tracking weight (δ) in ADAM’s anticipation module is a redundant parameter for synchronization with isochronous sequences, since both prediction (extrapolation) and tracking (perseveration) produce the same estimate for the next inter-stimulus interval. Anticipatory error correction (γ) did not independently produce an overall improvement in performance above and beyond that observed when adaptation was optimal, showing that it too, is not necessary for ideal performance with isochronous sequences.

Analysis of the lag-1 autocorrelation of the asynchronies revealed negative autocorrelation values when the total reactive error correction given by Eq. (12) was greater than one and was positive when the total reactive error correction was less than 0.99. Increasing anticipatory error correction did not alter this relationship except when $\gamma = 1$, where the autocorrelation was zero for all reactive error parameters

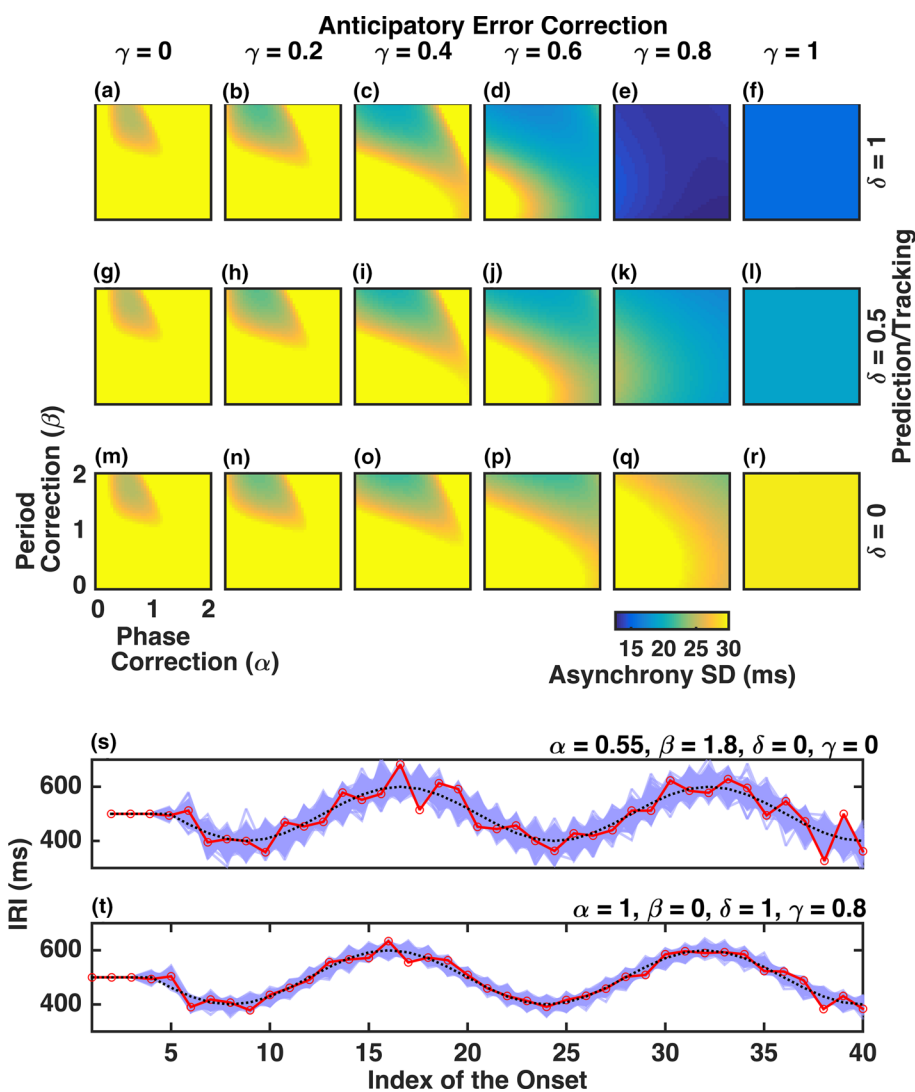
$$\text{Total reactive error correction} = \alpha + 0.5 \times \beta. \tag{12}$$

Cross-correlation of ISIs–IRIs was not possible for the steady tempo condition because the inter-stimulus intervals were identical for all intervals. A script for visualizing plots of the autocorrelation measures is available with the code accompanying this paper.

4.2.2 Tempo changes

Similar to the steady tempo simulation, the mean signed asynchrony failed to differentiate parameter settings that produced stable performance and will not be considered. In contrast, mean absolute asynchrony ranged from 9.83 ms upwards and the standard deviation of asynchronies ranged from 12.61 ms upwards across the various ADAM parameter settings for simulated synchronization with the tempo-changing sequence. Once again, the pattern of results for specific combinations of parameter settings was similar for mean asynchrony and the standard deviation of asynchronies, so only the standard deviation of asynchronies are presented. Each plot in Fig. 5 shows the standard deviation of asynchronies as a function of phase (*x*-axis) and period correction (*y*-axis) controlled by ADAM’s adaptation module. Each row depicts differing levels of prediction/tracking weight implemented by the anticipation module, with full extrapolation in the top row ($\delta = 1$), evenly balanced extrapolation and tracking ($\delta = 0.5$) in the middle row, and

Fig. 5 Effect of ADAM parameters on single-agent sensorimotor synchronization in the tempo change condition. **a–r** Standard deviation of asynchronies for the tempo-changing condition as a function of phase correction (x -axis), period correction (y -axis), prediction/tracking weight (rows), and anticipatory error correction (columns). **s, t** Inter-response interval for 250 simulations with the optimal parameter settings (blue) and the inter-stimulus onset of the tempo-changing sequence (red) for optimal parameter settings based on; reactive error correction alone (**s**) and with full extrapolation (prediction) and optimal anticipatory error correction (**t**) (color figure online)



full tracking ($\delta=0$) in the bottom row. Each column depicts differing levels of anticipatory error correction ($\gamma=0, 0.2, 0.4, 0.6, 0.8, 1$; left to right) in the joint module.

Focusing first on the reactive error correction settings when no anticipatory error correction was applied ($\gamma=0$; panels Fig. 5a–c), it can be seen that the standard deviation of asynchronies was lowest with period overcorrection ($\beta > 1$) combined with intermediate-to-low levels of phase correction. This suggests that (without anticipatory error correction) performance was optimized when overall reactive error correction mechanisms overcompensated for the most recent asynchrony to accommodate upcoming tempo changes in the stimulus sequence. Prediction/tracking (δ) settings did not modulate performance since the output of the anticipation module does not affect responses in the absence of anticipatory error correction ($\gamma=0$).

The effect of the prediction/tracking weight (comparing across rows) is only apparent when high levels of anticipatory error correction were applied ($\gamma > 0.5$; right columns),

with more subtle changes in stability observed for low levels of anticipatory error correction (left columns). When anticipatory error correction was low, increasing the prediction/tracking weight (bottom row, $\delta=0$; top row, $\delta=1$) generally improved overall performance without significantly altering the pattern of performance across the reactive error correction parameters. In contrast, for full anticipatory error correction (rightmost column; $\gamma=1$), reactive error correction no longer affected performance, and only the prediction/tracking weight altered synchronization precision (hence the uniform block of color in each panel).

Overall, it was clear that changes in anticipatory error correction had the largest impact on performance. Implementing anticipatory error correction ($\gamma > 0$) generally improved performance and modulated the extent to which reactive error correction (α, β) and the prediction/tracking weight (δ) influenced performance. The effect the anticipatory error correction on these parameters reflects how the joint module mediates the effect of the adaptation and

anticipation modules on behavior. Response timing is determined entirely by the output of the adaptation module (reactive error correction) when no anticipatory error correction is applied, and response timing entirely determined by the output of the anticipation module (prediction/tracking) when full anticipatory error correction is applied.

Ideal performance across all parameters (i.e., global minimum of the standard deviation of asynchronies) was observed with moderately high levels of anticipatory error correction ($\gamma=0.80$) in conjunction with full extrapolation (prediction, $\delta=1$) and maximum phase overcorrection ($\alpha=2$). The inclusion of prediction/tracking and anticipatory error correction parameters led to a substantial decrease in the standard deviation of asynchronies (12.61 ms, Fig. 5s) compared to the optimal parameter settings only involving reactive error correction (24.57 ms Fig. 5t), indicating that these parameters improve performance beyond what can be achieved by reactive error correction alone.

Analysis of the lag-1 autocorrelation of asynchronies demonstrated that the parameter settings that produced autocorrelation coefficients close to zero coincided approximately with parameter settings that minimized the standard deviation of the asynchronies (Fig. 6a–f). The prediction/tracking ratio (Fig. 6g–l) was greater than 1 for the majority of parameter settings, except for simulations where all parameter values were low, indicating that predictive inter-response intervals emerge with a surprisingly small degree of either reactive and/or anticipatory error correction. Moreover, the prediction/tracking ratio (PTR = 1.121) was highest when both anticipatory error correction and the prediction/tracking weight were set to 1.

4.2.3 Supplementary analysis: parameter separability/identifiability

Different parameter settings produced identical levels of performance across both steady tempo and tempo-changing simulations, suggesting overparameterization and potential problems with parameter identification. However, it is important to note that global measures of performance, such as the standard deviation of asynchronies, are only summary statistics for a pattern of asynchronies observed with each simulation trial and do not capture differences in the time-resolved pattern of asynchronies. For example, the steady tempo simulations with parameter settings of $\alpha=1.5, \beta=0$ (here we use the symbol θ_1 to represent a vector of parameter settings) and $\alpha=0.9596, \beta=0.5$ (θ_2) both produce a standard deviation of asynchronies of 11.4599 ms. However, the pattern of asynchronies produced by these two parameter vectors are not the same, indicating that these parameters are potentially separable, at least for modeling procedures that fit models to individual events (e.g., Jacoby and Repp 2012; Jacoby et al. 2015).

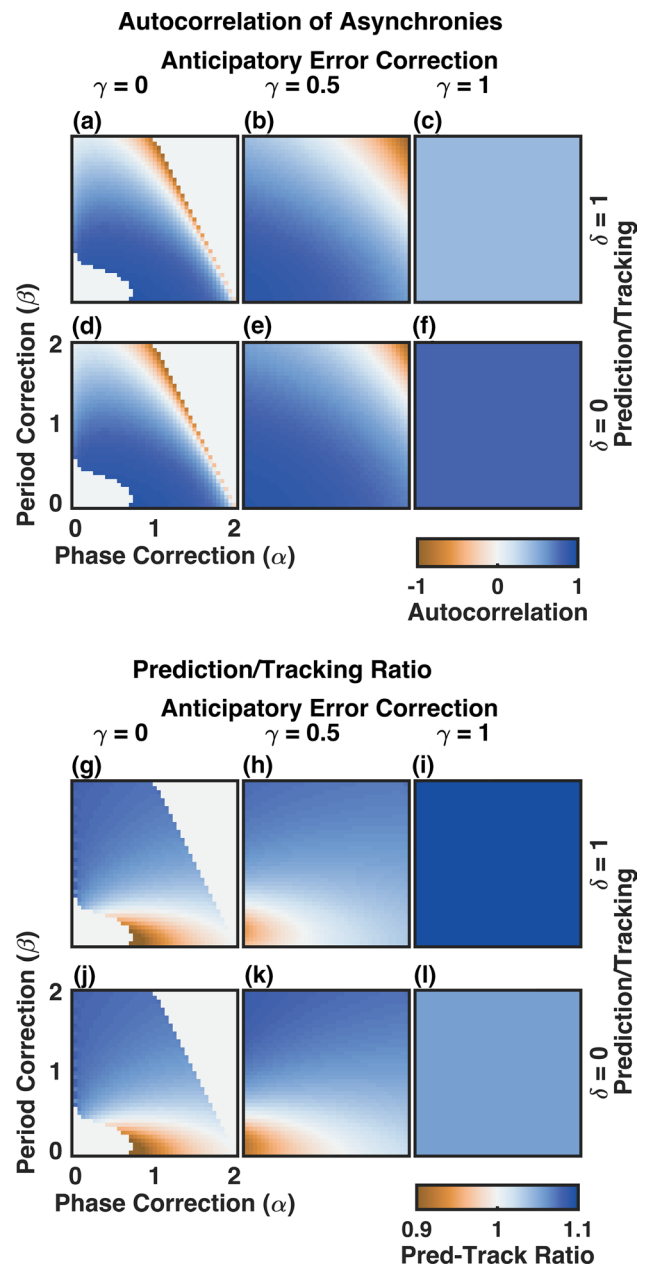


Fig. 6 Effect of ADAM parameters on the lag-1 autocorrelation and cross-correlation based measures in the single-agent, tempo change condition. **a–f** Lag-1 autocorrelation of the asynchronies as a function of phase correction (x-axis), period correction (y-axis), prediction/tracking weight (rows), and anticipatory error correction (columns). **g–l** Prediction-tracking ratio (based on lag-0 and lag-1 ISI–IRI cross-correlations) as a function of phase correction (x-axis), period correction (y-axis), prediction/tracking weight (rows), and anticipatory error correction (columns). Values corresponding to unstable performance (low or high reactive error correction) have been omitted

To formally examine the issue of parameter identifiability, we conducted a supplementary analysis that quantified the similarity of the pattern of asynchronies produced for a range of parameter settings. The similarity was defined as

the Euclidean distance between the vector of asynchronies produced for two parameter sets (θ_i and θ_j). The Euclidean distance was calculated for 1000 simulations where the noise vector was identical for both parameter vectors and varied across simulation trials. The total Euclidean distance was averaged across the 1000 simulations and entered into a parameter distance matrix. To help simplify the analysis, parameter identifiability was only assessed for two parameters at a time, thus for each analysis only two parameters were varied to create each parameter vector, with the remaining two parameters being fixed. Moreover, because parameter settings that produced very unstable performance also produced exponentially large asynchronies, only parameter settings that produced stable performance (standard deviation of asynchronies < 15 ms for steady tempo and < 25 ms for tempo change.) were included in the analysis.

Multi-dimensional scaling was used to visualize the first two dimensions of the distance matrix and was used to examine whether this procedure would recover the two-dimensional parameter space used to define parameter space. This analysis revealed that for the steady tempo condition, phase and period correction produced a two-dimensional manifold with parameter values organized topographically in a manner that roughly recovered the parameter space tested. In contrast, phase and anticipatory error correction produced a one-dimensional manifold, indicating that these two parameters are formally indistinguishable for the steady tempo condition. For the tempo-changing condition, only anticipation/tracking and anticipatory error correction were examined and were found to be separable when reactive error correction parameters were fixed at two different settings ($\alpha = 0.55$, $\beta = 1.8$ and $\alpha = 2$, $\beta = 0$). Although limited in scope, this analysis provides some evidence that the parameters are mostly separable except for anticipatory error correction under conditions of steady tempo. The scripts for this supplementary analysis can be found with the code accompanying this paper.

5 Dual-agent simulations

The aim of the dual-agent simulations was to explore the optimal coordination strategies when the task requires two bi-directionally coupled agents (agent 1 and agent 2) to synchronize their responses. Since previous studies have clearly outlined the role of reactive error correction mechanisms in adaptively timed and naturalistic scenarios (Repp and Keller 2008; Vorberg 2005; Wing et al. 2014), the primary goal was to determine the necessity of the mechanisms that comprise the anticipation and joint modules. As was the case in the single-agent simulations, the goal was to identify which parameter settings maximize synchronization stability by reducing the variability of the synchronization

error observed between the two agents' responses. Synchronization performance was again assessed for both steady tempo and tempo change conditions. By assessing performance with two interacting agents, the present simulations sought to understand what role the anticipation and joint modules play in a relatively complex, naturalistic context whereby each agent dynamically responds to their partner's performance.

Unlike single-agent simulations, where there are predefined inter-stimulus intervals that provide external synchronization targets, dual-agent simulations present a case where each agent provides the other's synchronization targets. This is unproblematic in the steady tempo case, as long as the internal timekeeper setting of each simulated agent matches the goal tempo. However, tempo-changing scenarios require at least one of the agents to have access to a target sequence of inter-onset intervals to serve as a goal. Therefore, a template-based approach, where each agent is given a series of temporal intervals as input prior to each trial, was employed to allow the simulated agents to produce the tempo-changing sequence from the single-agent simulation. Specifically, the model timekeeper was altered to store the pattern of inter-stimulus intervals from the tempo-changing sequence in a memory template, analogous to how musicians may have memory representations of a musical piece. These inter-stimulus intervals were used to plan the upcoming response by sequentially retrieving each inter-onset interval from memory.

The lack of an external target sequence in the dual-agent simulations also prompted us to devise additional measures of task performance to accommodate the implementation of the performance templates. Since both agents were able to mutually adjust their behavior to synchronize to their partner's actions, ideal performance (i.e., minimizing the standard deviation of asynchronies) could coincide with parameter settings where both agents depart from the sequence of intervals stored within their respective memory templates. Indeed, previous experimental work has shown that human piano duos that had learned incompatible sequences of tempo variations (prior to the experiment) tended to eschew the pattern of tempo change that they had practiced previously alone (prior to the experiment) in order to synchronize with their partner (MacRitchie et al. 2017). Thus, in the dual-agent simulations we sought to examine optimal parameter settings associated with two possible task goals from the perspective of each agent: (1) to synchronize with the other agent (i.e., inter-agent synchrony) and (2) to adhere to a partner's tempo goals determined by a template (see Fig. 7).

Measuring both joint and template-matching error variability allowed us to establish the importance of the leader–follower relationships within the broader range of strategies that were associated with ideal performance.

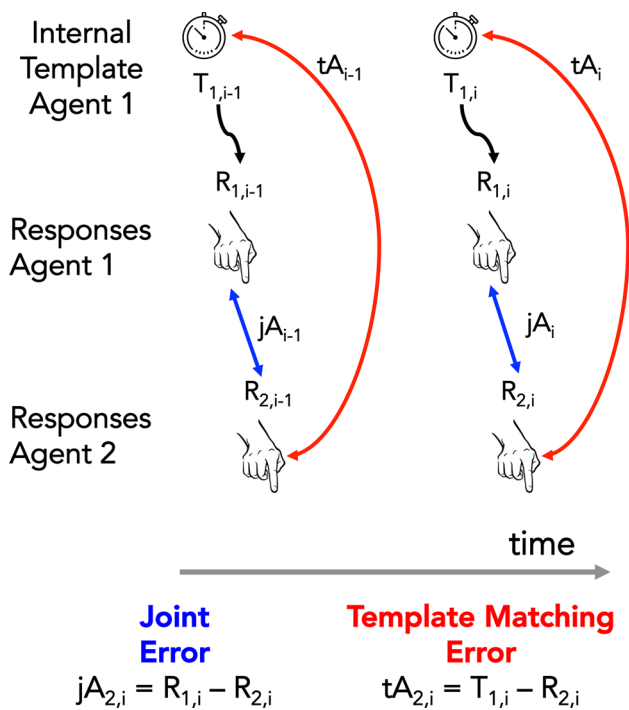


Fig. 7 Illustration of the joint error variability and template-matching error variability used to quantify performance in the dual-agent simulations. The sequence of inter-response intervals stored in the template for agent 1 (depicted as clocks) emits motor commands that trigger the agent 1’s responses. Joint error variability is calculated by subtracting the response onset times for agent 2 from agent 1 and then computing the standard deviation of these asynchronies for each trial. Template-matching error variability is calculated by subtracting the response onset times for agent 2 from the target response times for agent 1, as determined by the template

Whereas joint error variability exhaustively identifies all coordination strategies that produced stable performance (incorporating both asymmetrical, leader–follower strategies and symmetrical, balanced strategies), template-matching error variability specifically identifies coordination strategies that ensured that each agent followed their partners target performance. Thus, it was possible to determine whether asymmetrical coupling represented the ideal strategy for a particular task, or was merely one viable strategy out of a wider range of strategies.

Three dual-agent simulations were conducted to explore different tempo conditions. The first simulation examined the optimal coordination strategy when both agents were programmed to synchronize their responses with identical steady tempo performance templates. It was predicted that joint error variability would be minimized when the shared phase correction summed to 1 ($\alpha_1 + \alpha_2 = 1$). Based on previous research (Repp and Keller 2008; Vorberg 2005; Wing et al. 2014), we assumed that joint error variability would be minimized across a range of parameter combinations including symmetrical ($\alpha_1 \approx \alpha_2$) and asymmetrical

coupling strategies ($\alpha_1 < \alpha_2, \alpha_2 < \alpha_1$). However, in contrast, it was hypothesized that template-matching error variability would be minimized for asymmetric coupling strategies whereby phase correction was lower in the leader (agent 1) than the follower (agent 2). Given the results of steady tempo single-agent simulation, we further predicted that anticipatory error correction would not improve performance beyond that observed for optimal phase correction parameters.

The second dual-agent simulation assessed synchronization stability where both agents are programmed to produce the same pattern of tempo changes. Building on the finding from the single-agent simulation employing the tempo-changing sequence, we hypothesized that prediction/tracking and anticipatory error correction were necessary to optimize synchronization precision in the tempo-changing condition, we expected that ideal performance would be similar to that observed in simulation 1b. That is, ideal performance would be observed when each agent adopted optimal prediction/tracking ($\delta = 1$) and anticipatory error correction ($0.5 < \gamma < 1$). It was expected that optimizing joint error and template-matching error would produce the same results in this case, given that both agents were programmed to produce the same pattern of response intervals.

The final dual-agent simulation examined synchronization stability when both agents were programmed with incongruent performance templates, where agent 1 was programmed with tempo-changing performance template and agent 2 was programmed with a steady tempo performance template. The aim of these simulations was to examine how agents would negotiate an optimal coordination strategy when both agents were programmed with incompatible performance goals (e.g., MacRitchie et al. 2017). Of particular interest was whether the agents would engage in asymmetrical leader–follower coupling or symmetrical mutual coupling.

We assumed that template-matching error variability (relative to agent 1, implementing the tempo change template) would be minimized under highly asymmetrical parameter settings whereby agent 1 would adhere to their own performance template and ignore agent 2. On the other hand, agent 2 would integrate their partner’s performance into their own by anticipating the timing of agent 1’s action timing. Thus, we expected the template-matching error to be minimized when agent 1 implemented neither reactive nor anticipatory correction mechanisms ($\alpha_1 = \beta_1 = \delta_1 = \gamma_1 = 0$), effectively ignoring agent 2. Likewise, we expected ideal performance to coincide with when agent 2 incorporated predictions about agent 1’s performance into their responses. Similar to single-agent tempo-changing simulation, we assumed that ideal performance in this case would be observed when agent 2 implemented optimal anticipatory error correction ($\alpha_2 < 1; \beta_1 = 0; \delta_2 = 1; 0.5 < \gamma_2 < 1$).

In terms of minimizing the joint error variability, we expected that maximal synchronization stability would be

observed when both agents mutually adjusted their performance by partially incorporating predictions about their partner's response times into their performance. That is, we expected joint error variability to be minimized when each agent partially suppressed its own respective performance template and partially accommodated to their partner's performance by anticipating their action timing. Thus, we expected to observe ideal performance for simulations where each agent utilized high levels of prediction ($\delta_1 = \delta_2 = 1$) and intermediate levels of anticipatory error correction ($\gamma_1 = \gamma_2 = 0.5$).

5.1 Procedure

5.1.1 Dual-agent architecture, template implementation and performance measures

The dual-agent simulations comprised two interactive partners (agent 1, agent 2) that were each implemented with the ADAM architecture. The computations used to produce the responses were identical to those presented in the single-agent simulations with the exception that each partner now served as stimulus input for the other agent. That is, for agent 1 all references to the stimulus onsets (S_i) and stimulus intervals (s_i) were substituted for responses produced by agent 2 ($R_{2,i}$ and $r_{2,i}$). The equation for determining the joint errors for agent 1 ($A_{1,i}$) and agent 2 ($A_{2,i}$) are, respectively;

$$jA_{1,i} = R_{1,i} - R_{2,i} \quad (13)$$

$$jA_{2,i} = R_{2,i} - R_{1,i} \quad (14)$$

Furthermore, the equation used by agent 1 to predict the onset of the responses produced by agent 2 (and vice versa for agent 2) is;

$$S'_{1,i+1} = R_{2,i} + \delta_1 \times (2r_{2,i} - r_{2,i-1}) + (1 - \delta_1) \times r_{2,i+1} \quad (15)$$

$$S'_{2,i+1} = R_{1,i} + \delta_2 \times (2r_{1,i} - r_{1,i-1}) + (1 - \delta_2) \times r_{1,i+1} \quad (16)$$

The above procedure was implemented under three tempo conditions that varied in terms of the way in which timekeeper intervals were set and used to trigger responses. For the first simulation (steady tempo template), the interval stored in the timekeeper for both agents was initially set to 500 ms and remained constant throughout the trial unless altered by period correction. In the second simulation (tempo-changing template), both agents produced a predictable sequence of tempo variations that were retrieved from a template. In the third simulation (incompatible templates), agent 1 implemented a tempo-changing template and agent 2 implemented a steady tempo template.

The tempo-changing template sequence was identical to that used in the tempo-changing sequence from the

single-agent simulations. Template intervals (D_i) were implemented by setting the timekeeper value ($T_{1,i+1}$) used to plan the upcoming response ($R'_{1,i+1}$) equal to the next interval in the memory template (D_{i+1}) such that;

$$T_{1,i+1} = D_i = 500 + 100 \times \cos\left(\frac{(i-4) \times \pi}{8}\right) \quad (17)$$

Agents producing intervals according to the steady tempo template were implemented in the same manner as the single-agent simulations (Eq. 4).

We assumed that agents retrieving temporal sequences from memory have the capacity to accommodate to their partner's performance by shifting their overall global tempo (i.e., the average tempo) to better match their partner, while simultaneously maintaining local tempo variations associated with the memorized template. Computationally, this process of tempo scaling was implemented in the model by allowing period correction to be applied not only to the current timekeeper interval, but also to all upcoming intervals stored in the memory template.

Joint error variability was calculated by taking the standard deviation of the joint error (Eqs. 13, 14). The template-matching error variability was calculated by taking the standard deviation of the difference between the observed response onsets for agent 2 and the response onsets expected from the intervals stored in the internal template for agent 1 (and vice versa). The expected response onsets were calculated by taking the cumulative sum of all intervals from the start of the simulation trial to the current interval stored in the internal template $D_{1,i}$

$$tA_i = \sum_{i=4}^{64} (D_{1,i}) - R_{2,i} \quad (18)$$

5.1.2 Parameter search

Since the parameter space explored in the dual-agent simulations was much larger than the first set of simulations (8 vs. 4 parameters), we employed a two-step grid search technique to identify the optimal parameter settings. In the first step, parameter settings for both agents were systematically varied to identify parameter combinations that minimized joint error variability and template-matching error variability. Phase and period correction parameter values for each agent were sampled from within the range of 0–1 with an interval of 0.5. Likewise, the prediction/tracking weight and the anticipatory error correction parameter values were sampled from the range of 0–1 with an interval of 0.5. Timekeeper noise was held at a constant value of 10 ms for both agents across all simulations. Both joint error variability and template-matching error variability

calculated for each simulation were averaged over 1000 trials per parameter combination.

To evaluate the role that each parameter played in producing ideal performance at this first step, we ran a correlation analysis on the optimal parameter settings to identify any inter-relationships between the parameters. This analysis identified three generic types of parameter: fixed parameters, redundant parameters, and complementary parameters. Fixed parameters did not correlate with the other parameters and adopted only a single value across the simulations that yielded ideal performance. Redundant parameters also did not correlate with any other parameters but differed from the fixed parameters in that all simulated values were associated with the minimal error measure. Finally, complementary parameters demonstrated a negative correlation with other parameters, indicating that ideal performance could be maintained if the two agents adopted complementary parameter settings (i.e., parameter settings traded-off between agents).

At a second step, to provide a more fine-grained picture of the relationship between these interrelated parameters, we performed additional simulations to explore the parameters identified as complementary in the correlation analysis with increased resolution by running simulations for all parameter settings between 0 and 1 sampled in steps of 0.02.

5.2 Results

5.2.1 Dual-agent, steady tempo template

The steady tempo templates simulation examined synchronization performance when the two virtual agents were programmed to produce a steady tempo sequence. Initial simulations revealed 27 parameter combinations that shared the same minimal joint error variability. The standard deviation of the joint error variability was lowest when phase correction had complementary settings across the two agents ($\alpha_1 + \alpha_2 = 1$), period correction was fixed at zero for both agents ($\beta_1 = \beta_2 = 0$), the prediction/tracking weight (δ_1 and δ_2) varied freely (indicating redundancy in the sense that all parameter values were optimal), which was due to anticipatory error correction being found to be fixed at zero ($\gamma_1 = \gamma_2 = 0$).

Follow-up analysis focusing only on variation of phase correction for both agents is shown in Fig. 8a, b. This analysis revealed minimal joint error variability when phase correction summed across both agents was 0.98 (Fig. 8a). Standard deviation of asynchronies for the optimal parameter settings was found to be 14.09 ms, which is slightly less than the minimal variability expected from the current simulations based on the timekeeper noise settings (combined timekeeper variability, 14.14 ms).

Complementary phase correction is consistent with previous studies (Repp and Keller 2008; Vorberg 2005; Wing

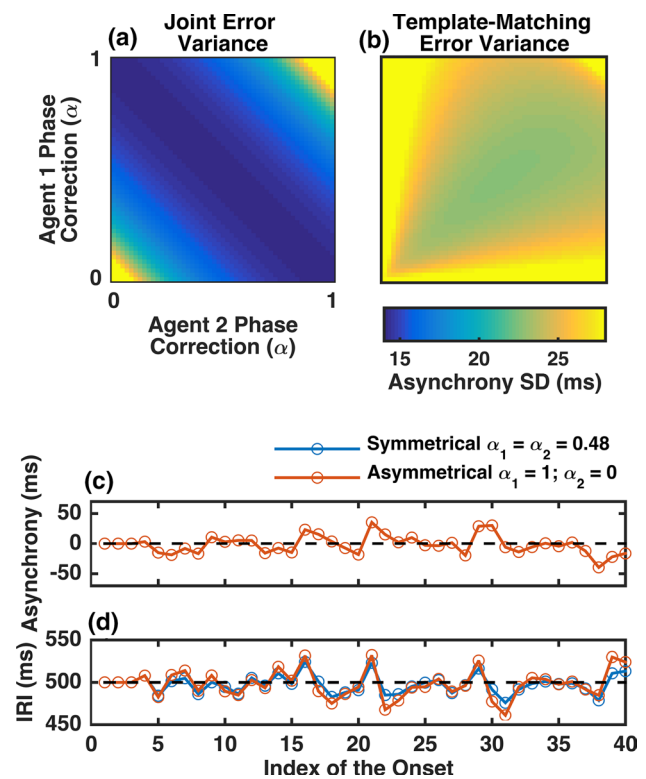


Fig. 8 Measures of synchronization stability for dual-agent simulations in the steady tempo condition. **a** Joint error variability, **b** template-matching error variability as a function of the amount of phase correction (α) employed by agent 2 (x-axis) and agent 1 (y-axis). The joint error plot shows ideal performance for complementary phase correction for agents 1 and 2 summing to approximately 0.98, whereas the template-matching error indicates ideal performance when both agents adopted similar, intermediate phase correction values. **c** Representative asynchrony timecourse, **d** inter-response intervals (bottom panel) for agent 2 under a symmetrical (blue) and asymmetrical (red) phase correction settings. Although symmetrical and asymmetrical parameter combinations produced similar asynchrony plots, the inter-response interval produced for the symmetrical parameter settings was less variable than the asymmetrical parameter settings, implying steadier tempo was maintained with symmetrical parameter settings (color figure online)

et al. 2014), showing ideal performance when synchronization errors are almost completely corrected across both agents. As observed in previous studies (Repp and Keller 2008), ideal performance was achieved with slightly less than full phase correction ($\alpha_1 + \alpha_2 < 1$). This may be the case because local variability associated with some portion of internal noise does not require correction, although this explanation is based on simulations that modeled motor noise (Vorberg and Schulze 2002), which was not included in the present simulations. Therefore, it may instead be the case that variability associated with the interaction partner provides a source of noise that cannot be fully accounted for by phase correction.

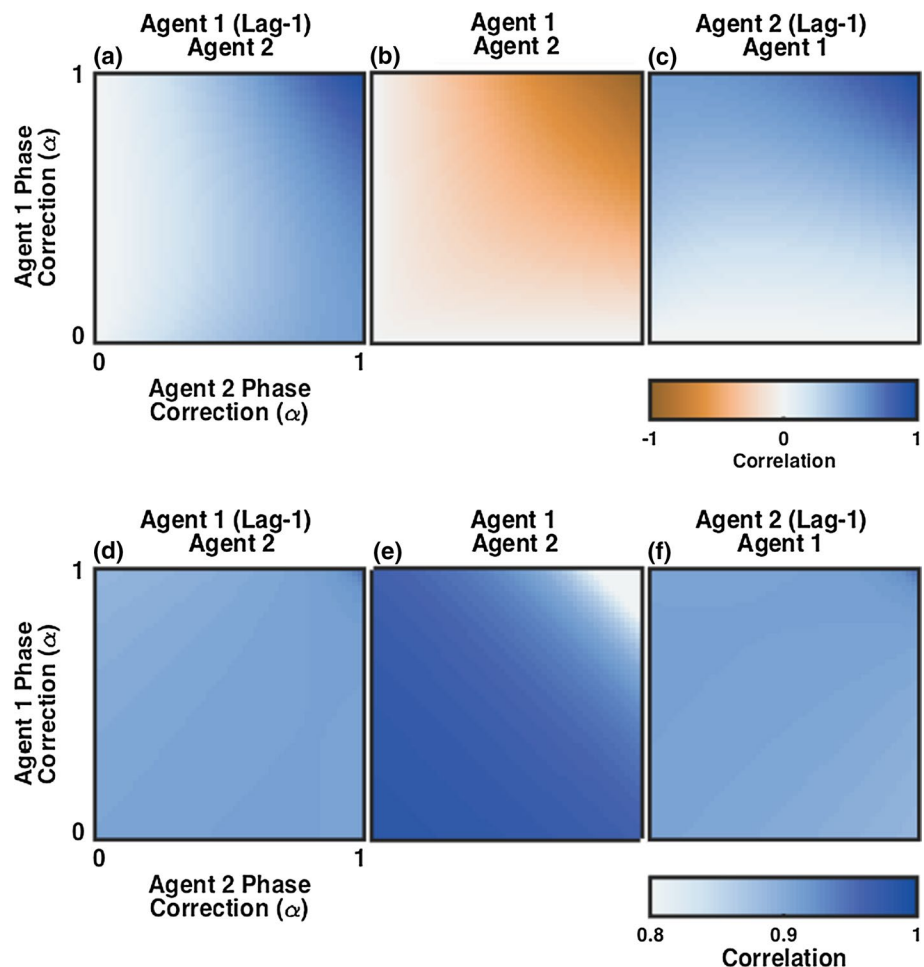
For the template-matching error, the initial simulations identified 9 parameter settings associated with stable synchronization. Most parameters for these simulations were fixed, with phase correction for each agent (α_1 and α_2) set to 0.5, and period correction (β_1 and β_2) and anticipatory error correction (γ_1 and γ_2) set at 0. The prediction/tracking weight (δ_1 and δ_2) was again found to be redundant. Detailed analysis of phase correction and template-matching error variability revealed (Fig. 8b) that template-matching error variability was minimized when both agents adopted almost identical, intermediate levels of phase correction ($\alpha_1 = 0.48$, $\alpha_2 = 0.50$). The minimal template-matching error variability for the optimal parameter settings was found to be 22.70 ms with a corresponding joint error variability of 14.09 ms.

Consistent with results for single-agent synchronization at a steady tempo, the results of the present dual-agent simulation indicate that phase correction alone is sufficient for ideal performance in contexts requiring regular timing. Moreover, whereas joint error variability was minimized under both asymmetrical (leader–follower) and symmetrical correction strategies, minimizing template-matching error variability—thus maintaining a steady tempo throughout the

interaction—was only achieved when both agents symmetrically employed intermediate levels of phase correction. Figure 8c, d makes this point clear, where the top panel (Fig. 8c) shows that both symmetrical and asymmetrical parameter settings produce almost identical asynchrony time series, whereas the inter-response intervals (produced by agent 2) show reduced variability for symmetrical compared to asymmetrical parameter settings (Fig. 8d). Taken together, these results suggest that a symmetrical dyadic interaction minimizes the variability of observed asynchronies and ensures that both agents maintain the initial tempo.

The lag-1 autocorrelation of the asynchronies showed a similar relationship as found in the single-agent simulation, where the autocorrelation was negative when the sum of the phase correction values was greater than 0.98, and transitioned to increasingly positive values as the sum of phase correction values decreased. The cross-correlations between IRIs of agent 1 and agent 2 (Fig. 9a–c) showed more positive correlations at lag-1 when a partner implemented greater phase correction. That is, an agent's IRIs lagged behind their partner's IRIs when the former agent adopted high levels of phase correction (Fig. 9a, c). The most positive

Fig. 9 Cross-correlations of the IRIs produced by agents 1 and 2 in the steady tempo (a–c) and the tempo change, congruent template conditions (d–f) as a function of the phase correction (α) employed by agent 2 (x-axis) and agent 1 (y-axis). **a, d** Correlation between agent 2's IRIs and the lagged IRIs of agent 1 (lag-1). **b, e** Correlation between the IRIs of agents 1 and 2. **c, f** Correlation between agent 1's IRIs and the lagged IRIs of agent 2 (lag-1). Note the different scale used for the steady tempo (minimum = -1; maximum = 1) and the tempo change (minimum = 0.8; maximum = 1) simulations



lag-1 IRI cross-correlations were observed when both agents implemented high levels of phase correction ($r=0.94$). The lag-0 cross-correlation was close to zero when either agent implemented no phase correction, and became more negative as agents implemented more phase correction (Fig. 9b), with the lowest value observed for full phase correction ($r=-0.96$). The pattern observed for the IRI cross-correlations was consistent with the notion of hyper-followers in steady tempo tasks, whereby lag-1 measures are positive and lag-0 measures are negative (Konvalinka et al. 2010).

5.2.2 Dual-agent, tempo-changing template

The results of the simulations where both agents were programmed to produce identical tempo-changing sequences were almost identical to the results observed in the simulations involving two agents programmed to produce a steady tempo. Optimal joint error variability was observed for 27 simulations where phase correction (α_1 and α_2) was observed to be a complementary parameter, prediction/tracking weighting was a redundant parameter, and both period and anticipatory error correction were found to be fixed-zero parameters. Follow-up analysis of the phase correction parameters revealed that joint error variability was minimized when the total phase correction summed to 0.98. Standard deviation of asynchronies for the optimal parameter settings was found to be 14.09 ms. Thus, in contrast to the single-agent, tempo-changing simulation, where the prediction/tracking weighting and anticipatory error correction were necessary for ideal performance, the present dual-agent results suggest that prediction/tracking and anticipatory error correction are not required in a tempo-changing context when both agents share a representation of the target performance.

Analysis of the template-matching error variability also exhibited the same pattern as the steady tempo condition. The grid search technique revealed 9 parameter settings that minimized template-matching error variability, with phase correction found to be a fixed parameter ($\alpha_1 = \alpha_2 = 0.5$), prediction/tracking weight a redundant parameter, and both period and anticipatory error correction fixed-zero parameters. Detailed analysis of the phase correction settings showed that the template-matching error variability was minimized when both agents adopted intermediate levels of phase correction (e.g., $\alpha_1 = 0.48$; $\alpha_2 = 0.50$). Importantly, inspection of the inter-response intervals produced by each agent closely matched the temporal intervals stored in the performance template (Fig. 10a) for the optimal parameter settings. Minimal template-matching error variability was again found to be 22.7 ms (corresponding joint error variability, 14.09 ms).

The lag-1 autocorrelation of the asynchronies showed the same relationship as in steady tempo dual-agent

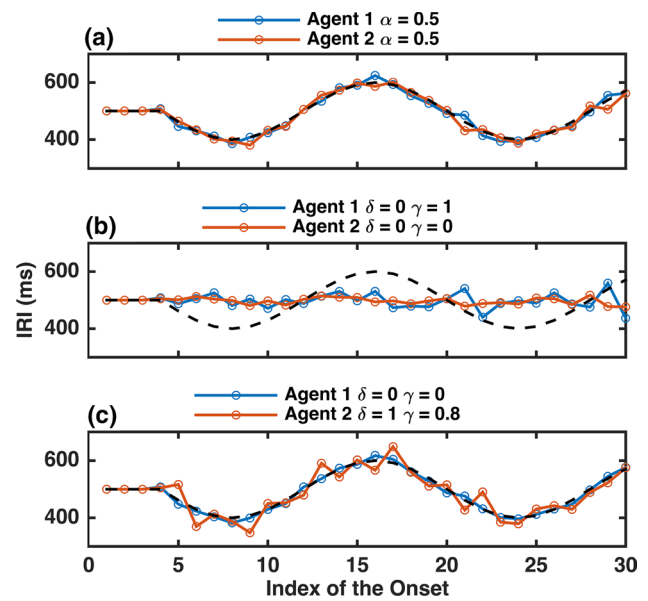


Fig. 10 Inter-response intervals produced by agent 1 and agent 2 for the congruent (a) and incongruent template conditions (b, c) in the dual-agent simulations. Panels depict representative trials for the parameter settings that minimize joint error variability for the congruent and incongruent template conditions (a, b) and the template-matching error variability (c). The black dotted line represents the temporal intervals stored in the tempo change template (implemented in agent 1 in b and c)

simulation, negative correlations when the sum of the phase correction values was greater than 0.98, and transitioned to increasingly positive values as the sum of phase correction values decreased. Unlike the steady tempo condition, the IRI cross-correlations (Fig. 9d–f) were positive at all lags (1, 0, and -1). Nevertheless, the qualitative pattern of results was similar to the steady tempo, dual-agent simulation. The lag-1 (Fig. 9d, f) correlations were highest when both agents adopted full phase correction ($r=0.94$). Likewise, the lag-0 correlations (Fig. 9e) were highest when both agents did not engage in phase correction ($r=0.98$) and were lowest when both agents adopted full phase correction ($r=0.13$; note the scale was truncated for Figs. 9d–f to emphasize differences in correlations values for the lag-1 measures). The inflated cross-correlations exhibited in the current simulation was likely due to the tempo-changing intervals contributing the largest source of variance in the pattern of the IRIs, which was shared by both agents. This contrasts with the steady template condition where variation in the IRIs would have reflected only noise perturbations from the timekeeper of each agent. Although timekeeper noise also would have contributed to variability in the tempo change simulation, this would have made up a smaller proportion of the variability compared to the tempo-changing performance template.

5.2.3 Dual-agent, incompatible template

Simulations comprising two agents each implementing incongruent performance templates (agent 1, tempo change; agent 2, steady tempo) revealed 27 simulations that minimized the joint error variability. These showed that joint error variability was minimized when all reactive and anticipatory correction parameters for agent 2 were set to zero (i.e., agent 2 anticipation/tracking parameter was redundant), and when agent 1 adopted a full tracking strategy ($\delta_1 = 0$, $\gamma_1 = 1$, wherein all reactive error correction parameters were redundant as anticipatory error correction was set to maximum). Thus, an inter-agent coordination strategy that stabilizes joint error in the context of incompatible tempo goals (changing versus steady tempo) is associated with agent 1 abandoning their tempo-changing performance template and mirroring the behavior of the agent producing a steady tempo (Fig. 10b). The joint error variability observed for these parameter settings was 17.3 ms. These parameter settings coincided with a lag-1 autocorrelation of asynchronies of -0.34 , and a lag-1 cross-correlation between the IRIs of agent 1 and 2 of 0.75 , with all other cross-correlation values close to zero, indicating that agent 1 was effectively tracking agent 2.

A different pattern of results emerged for the case that involved minimizing template-matching error variability. Initial simulations revealed 27 parameter settings that minimized template-matching variability, all comprising reactive and anticipatory error correction set to zero for agent 1, and anticipatory error correction set to one and prediction/tracking weighting set to 0.5 for agent 2. Detailed parameter search wherein parameters for agent 1 were fixed to zero showed that template-matching error was minimized when agent 2 implemented full anticipatory weighting and high anticipatory error correction ($\delta_2 = 1$; $\gamma_2 = 0.8$) with no reactive error correction ($\alpha_2 = \beta_2 = 0$). Under these conditions, agent 2 produced a sequence of inter-response intervals that closely matched the inter-response intervals produced by agent 1 (Fig. 10c). These results indicate that asymmetrical coupling is required to ensure that both agents produce the tempo-changing sequence under conditions where the one agent does not share the tempo-changing performance template. The minimal template-matching error variability observed for the optimal parameter settings was 38.0 ms (and a corresponding joint error variability of 22.87 ms). The parameter settings that produced minimal template-matching error variability for agent 1 were identical to the parameter settings that minimized the joint error variability between both agents. The optimal template-matching parameter settings produced a lag-1 autocorrelation of asynchronies of -0.20 , and uniformly high (i.e., > 0.8) cross-correlation values with the lag-0 IRI cross-correlation coefficient exhibiting the highest value (agent 1 lag-1 IRI \times agent

2 IRI = 0.89 ; agent 1 \times agent 2 IRI = 0.9 ; agent 1 \times agent 2 lag-1 IRI = 0.81). The resultant prediction/tracking ratio of 1.01 indicates that these parameter settings produced weakly predictive IRIs for agent 2.

6 Discussion

The present study investigated the role of different parameters in ADAM, a linear event-based model of sensorimotor synchronization (Keller et al. 2016; van der Steen et al. 2015a; van der Steen and Keller 2013), using computer simulations of unidirectional, single-agent synchronization with a pacing sequence (such as when a musician synchronizes with a metronome or a recording) and dual-agent interaction under steady tempo and tempo-changing conditions. A range of parameter combinations were tested in order to determine which parameters from ADAM's adaptation, anticipation, and joint modules are necessary for maximizing stable sensorimotor synchronization performance, defined as minimizing the variability (standard deviation) of asynchronies. Results generally indicated that reactive error correction parameters in ADAM's adaptation module were influential across tempo and interaction conditions. In contrast, the parameters governing the balance between prediction and tracking in the anticipation module, and the anticipatory error correction parameter in the joint module, were only influential under tempo-changing conditions.

Two sets of optimal parameter settings emerged consistently across the single- and dual-agent simulations. The first was most clearly identified in the steady tempo condition. Under both single- and dual-agent conditions, ideal performance in the steady tempo condition was determined exclusively by the phase correction setting. Period correction, prediction/tracking weighting, and anticipatory error correction exerted no influence under these conditions. Whereas ideal performance in the single-agent condition was observed when the simulated agent adopted full phase correction, optimal phase correction in the dual-agent simulations depended on whether performance success was quantified on the basis of inter-agent joint synchrony or adherence to an interaction partner's tempo goals predetermined by a template.

When performance was quantified as the variability observed in inter-agent asynchrony (joint error variability), ideal performance coincided with total phase correction employed by both agents summing to 0.98 . In contrast, when performance was quantified as the variability of the synchronization error between the performance template implemented in agent 1 and the responses produced by agent 2 (template-matching error variability), ideal performance was observed when both agents adopted intermediate levels of phase correction. This finding indicates that

whereas minimizing inter-agent synchronization error (i.e., joint error variability) can be achieved by either adopting an asymmetrical (i.e., leader–follower) or symmetrical inter-agent coordination strategy, maintaining a steady tempo (low template-matching error) is observed only when both agents implement equal phase correction (i.e., symmetrical interpersonal coordination strategy). Intriguingly, the same pattern of results was also observed in the dual-agent simulations where both agents implemented identical tempo-changing performance templates. Only phase correction was necessary to obtain ideal performance, with shared phase correction equaling 0.98 again minimizing joint error variability, and shared intermediate phase correction minimizing template-matching error variability. Taken together with the steady tempo simulations, these results suggest that optimizing phase correction parameter settings reflect the best interpersonal coordination strategy when both agents share a common performance template. This supports the assumption that, in the case of musical ensemble performance, interpersonal coordination can be achieved relatively automatically if co-performers possess a shared representation of expressive timing goals related to the ideal ensemble sound (Keller 2008; MacRitchie et al. 2017a; cf Schiavio and Høffding 2015).

The second set of optimal parameter settings identified in the current study was observed in relation to the tempo-changing condition. Maximally stable performance in the single-agent tempo-changing condition was observed when the agent implemented a full extrapolation (prediction) and moderately high anticipatory error correction. Similar results were observed in the dual-agent simulations, however only for the incongruent templates condition where one agent implementing a steady tempo performance template interacted with a partner implementing a tempo-changing performance template. Here, template-matching error variability was minimized when the agent implementing the steady tempo template adopted full extrapolation (prediction) and moderately high anticipatory error correction. This highlights the benefits of asymmetrical leader–follower relations specifically in the case of negotiating tempo changes (while such relations may be detrimental at a steady tempo; Novembre et al. 2015; Vorberg and Schulze 2002). Asymmetrical relations are generally beneficial under conditions of high task difficulty during interpersonal coordination (Skewes et al. 2015). In a musical duo situation where one individual is committed to producing specific patterns of tempo variation (for example, a soloist with preplanned expressive intentions playing with an accompanist), temporal prediction and anticipatory error correction should be required primarily on the part of the co-performer (the accompanist).

The dual-agent simulations also revealed another optimal parameter setting that was not observed in the single-agent simulations and are thus informative about potential

coordination strategies in mutually coupled interactions. For the incongruent tempo condition, ideal inter-agent synchronization stability (joint error variance) was observed when agent 2 (steady tempo template) implemented neither reactive nor anticipatory error correction, and agent 1 (tempo change template) implemented full tracking and anticipatory error correction parameter settings. The result of this parameter setting was agent 1 abandoning their tempo-changing template to synchronize with the steady tempo performance produced by agent 2. Complete adoption of the steady tempo performance by agent 1 presumably reflects the fact that tempo variations associated with the tempo-changing template are inherently less stable in comparison with the simpler task of maintaining a steady tempo. In a musical duo scenario, this could amount to the soloist abandoning their expressive timing goals and playing at a deadpan metronomic tempo dictated by the accompanist (presumably not an ideal state of affairs).

Taken together, the single- and dual-agent simulations provide novel insight into the role that each of ADAM's parameters plays in sensorimotor synchronization under conditions emphasizing tempo maintenance and tempo change. In what follows, we discuss the implications of these findings for each module in the model, first discussing the reactive error correction parameters in the adaptation module, and then the prediction/tracking weight from the anticipation module and the anticipatory error correction implemented by the joint module.

6.1 Adaptation module

The adaptation module comprises phase and period correction, two reactive error correction mechanisms that are standard components of traditional autoregressive models of sensorimotor synchronization. Consistent with previous studies (Repp and Keller 2008; Repp et al. 2012; Wing et al. 2014), phase correction was found to play an important role in simulations involving maintenance of a steady tempo, with optimal phase correction corresponding to parameter settings where the total sum of phase correction applied was 0.98. In the single-agent, steady tempo condition, complete phase correction produced a standard deviation of asynchrony that was equal to the timekeeper noise setting used in the simulations, confirming that optimal phase correction can fully accommodate the timing error associated with the timekeeper (see Vorberg and Schulze 2002; Wing et al. 2014). Period correction, in contrast, generally had a deleterious effect on synchronization stability in the steady tempo condition. Period correction in this condition allowed the timekeeper to drift from the tempo initially set by the stimulus sequence at the start of each simulated trial, which increases performance variability (see also Repp and Keller 2008). This implies that investing effort when synchronizing

at a steady tempo, by attempting to compensate for what are essentially random timing fluctuations, may in fact be detrimental to achieving temporal goals.

Both period and phase correction played a positive role in producing ideal performance in the tempo change condition. Period overcorrection in conjunction with moderate phase correction produced reasonably stable synchronization for the tempo-changing sequences. By overcorrecting the most recent asynchrony, parameter settings employing a high degree of period correction are capable of accommodating changes in the tempo of the stimulus sequence. That is, by employing period overcorrection, the timekeeper interval can be set larger (or smaller) than the most recent inter-stimulus interval, and thus accommodate upcoming changes in the stimulus sequence by overcompensating for recent errors. For example, if the tempo is slowing (increasing inter-stimulus intervals) taps will tend to be early. Period overcorrection will lengthen the next inter-response interval so that it will be larger than the most recent inter-stimulus interval. The resulting inter-stimulus interval produced by period overcorrection will be a closer match to the next inter-stimulus interval, which will also be longer than the most recent inter-stimulus interval. Previous work has found that human participants display behavior that is consistent with phase overcorrection in the context of synchronization with tempo-changing sequences (van der Steen et al. 2015a). The current results suggest that period correction may be an alternative strategy that can be consciously applied, albeit with effort (see Repp and Keller 2004).

The ideal combination of phase and period correction in the tempo-changing condition was altered by the degree to which anticipatory error correction was employed, and by whether both agents shared the same performance template. In the single-agent simulation, period overcorrection and moderate phase correction were required for ideal performance when levels of anticipatory error correction were low. However, period correction was no longer necessary to produce ideal performance, and reactive error correction only required phase correction when anticipatory error correction was optimal. Likewise, only phase correction was required when both agents employed the same tempo change template. This would be the case in musical scenarios where co-performers possess similar representations of expressive timing goals (Keller et al. 2014), acquired over the course of ensemble rehearsal as the musicians become increasingly familiar with the musical piece and each others' idiosyncratic playing styles (MacRitchie et al. 2017a; Ragert et al. 2013; Repp and Keller 2010).

The use of either phase or period correction presumably reflects the optimal strategy for dealing with variability induced by the stimulus sequence (i.e., tempo changes) and internal noise (i.e., timekeeper noise). When the anticipation module cannot provide accurate estimates of the stimulus

onsets (such as when tempo acceleration turns into tempo deceleration), or the joint module does not correct enough of the predicted error, period correction becomes effective by reactively accommodating the changes in the stimulus sequence. This situation could arise when ensemble performers are faced with an unfamiliar piece or an unfamiliar partner, making the process of achieving interpersonal coordination effortful. However, when the change in tempo is accommodated by the optimal prediction/tracking and anticipatory error correction settings, only phase correction is necessary to provide a local adjustment to deal with variability associated with the timekeeper. A familiar partner or well-rehearsed performance may thus allow the use of templates that reduce attentional load.

Taken together, the mechanisms implemented in ADAM's adaptation module are necessary to produce ideal performance across a range of conditions. Phase correction plays a ubiquitous role in sensorimotor synchronization to correct sources of internal noise (i.e., timekeeper noise) both when the tempo must be maintained and during periods of tempo change. This is consistent with the automatic and obligatory nature of phase correction (Repp 2001; Repp and Keller 2004; Schulze et al. 2005), suggesting that this fundamental mechanism of entrainment is necessary for interpersonal coordination (Keller et al. 2014; Phillips-Silver et al. 2010). In musical contexts, phase correction may be sufficient when the tempo is steady and when co-performers have matching goals in terms of tempo changes. In situations where phase correction is not sufficient, period overcorrection is beneficial for dealing with tempo changes. The adaptation module alone can produce reasonably stable performance in tempo-changing sequences. However, the adaptation module is purely reactive and driven by asynchronies. By itself, this module cannot detect nor exploit systematic timing patterns present in the stimulus sequence to plan future responses.

6.2 Anticipation and joint modules

ADAM's anticipation and joint modules are relatively novel constructs insofar as traditional linear error correction models (e.g., Mates 1994a; Vorberg and Schulze 2002; Vorberg and Wing 1996) and nonlinear dynamical systems models (e.g., Dumas et al. 2014; Kelso et al. 2009; Loehr et al. 2011) do not incorporate equivalent processes. While previous empirical work suggests that these new modules are valid psychological constructs (van der Steen et al. 2015a), the way in which they interact with one another and with reactive error correction had not been previously explored. Specifically, although a previous study that included simulations (van der Steen et al. 2015a) did examine the anticipation/tracking weight, this was done only to explore inter-relationships with reactive error correction and did not entail a detailed examination of anticipatory error

correction. Moreover, these simulations were only based on tempo-changing sequences, leaving open the question of whether the anticipation and joint modules are beneficial for sequences with no changes in tempo.

The anticipation module in ADAM provides an estimate of future stimulus events based on patterns recently observed in the stimulus sequence, whereas the joint module estimates the predicted asynchrony between the outputs of the adaptation and anticipation modules, and provides anticipatory error correction in advance of action execution. Although separate modules, the effect of the predicted stimulus onsets provided by the anticipation module are essentially gated by the level of anticipatory error correction employed by the joint module, thus the function of the two parameters from these modules will be discussed together.

As expected, the effect of the prediction/tracking weight and the anticipatory error correction parameters was most apparent in the context of tempo changes. In the single-agent condition, ideal performance was observed for simulations employing full extrapolation (prediction) and intermediate-high anticipatory error correction. The benefits of temporal prediction are consistent with a growing body of behavioral results (e.g., Mills et al. 2015; Pecenka and Keller 2011; Repp 2002) and, while anticipatory error correction is less thoroughly examined, previous work with ADAM suggests that versions of ADAM that include it account well for observed behavior with tempo-changing sequences (van der Steen et al. 2015a; van der Steen et al. 2015b).

There are two reasons why ideal performance coincides with this combination of parameter settings. Firstly, the anticipatory error correction parameter mediates the influence of the adaptation and anticipation modules on the behavior of the model (van der Steen et al. 2015a). For full anticipatory error correction, the response onsets produced by the model are identical to predicted stimulus onsets produced by the anticipatory module. The drawback associated with this parameter setting (in which the adaptation module is silent) is that the model has no capacity to reactively correct for effects of local noise.

The second way in which intermediate levels of anticipatory error correction contributes to ideal performance is by compensating for systematic inaccuracies associated with the anticipatory module. The anticipatory module provides estimates of future stimulus onsets through either an inaccurate tracking process (for tempo-changing sequences) or a more accurate extrapolation process. Although the extrapolation process provides relatively accurate estimates of the inter-stimulus interval when tempo changes in a consistent manner, extrapolation cannot provide accurate estimates of stimulus onsets when the rate of change in the tempo is altered, such as at turning points in the tempo-changing sequence. Thus, adopting an intermediate amount of anticipatory error correction also ensures that errors in the

predicted stimulus onsets can be compensated for by reactive error correction mechanisms. In psychological terms, this amounts to the partial integration of information in internal models of ‘self’ and ‘other’ (Keller et al. 2016). In musical contexts, balancing self-other integration and segregation may be optimal to the extent that it allows co-performers to monitor the joint action outcome while maintaining a distinction between self and other, which enables each performer to retain autonomous control of their own movements (Keller et al. 2014; Novembre et al. 2016).

The results of the dual-agent simulations also provide new insights into the importance of the anticipation and the joint modules in rhythmic forms of joint action. Neither the prediction/tracking weight nor anticipatory error correction was necessary in the simulations where both agents employed the same tempo-changing performance template. Instead, the anticipation and joint modules only played a role in producing ideal performance when the agent implementing a steady tempo template attempted to produce the tempo-changing template implemented by their interaction partner. Since it is assumed that adaptation and anticipation provide input for self and other internal models, these results are consistent with the notion that shared representations modulate the relative focus on self and other in joint action contexts (Keller et al. 2016). In musical situations where co-performers possess a shared representation of an interaction goal, such as when playing a well-practiced piece of ensemble music (Ragert et al. 2013; Novembre et al. 2016), presumably little attention needs to be directed to other individual’s performance and more attention can be directed to technical and expressive aspects of one’s own performance. In situations where shared representations are less likely, as in musical improvisations where novel melodic and rhythmic material is created on the fly, co-performers may rely more on online anticipatory processes, and hence an increased focus on each other’s performance, in order to integrate predictions about others’ upcoming actions with one’s own action plans.

Finally, the single-agent simulations revealed an important limiting case when applying ADAM to data collected from stimulus sequences comprising isochronous intervals. Under steady tempo conditions, the anticipatory error correction parameter was shown to produce identical time-resolved behavior as the phase correction parameter, indicating overparameterization and problems with parameter separability and identifiability in this context. However, overparameterization was only present in the steady tempo conditions involving an isochronous sequence and was not present in the steady tempo, dual-agent simulation where anticipatory error correction was not identified as a necessary parameter. This suggests that when used in laboratory experiments where stimulus sequences are typically programmed to be completely isochronous, it is appropriate to use only the traditional reactive error correction models to

quantify the latent sensorimotor mechanisms employed by participants. For sequences that contain tempo variations, such as those found in naturalistic interactions (i.e., musical performance), it is especially informative to compare the fit produced by ADAM against simpler models employing only reactive error correction (e.g., van der Steen et al. 2015a).

6.3 Implications

In addition to having a didactic role in illuminating ADAM's functional properties, the results of the present simulations hold potential implications for basic and applied questions in fields including cognitive neuroscience, psychology, music pedagogy, neurology, and human–machine interaction.

Implications for cognitive neuroscience and psychology derive from the possibility to estimate parameters related to each ADAM module from the behavior of human participants. With regard to cognitive neuroscience, identifying the network of brain regions associated with each ADAM module, and analyzing patterns of functional connectivity between these networks, will advance our understanding of the neural bases of sensorimotor and cognitive skills that enable precise yet flexible interpersonal coordination. With regard to psychology, the ways in which ADAM's adaptation, anticipation, and joint modules interact can potentially inform our understanding the sources of individual differences in sensorimotor synchronization skill. Previous work has identified links between different dimensions of personality and processes instantiated in ADAM's adaptation and anticipation modules (Fairhurst et al. 2014; Keller et al. 2014; Novembre et al. 2014; Pecenka and Keller 2011). Examining how the interactions between these modules, as revealed by the present simulations, are linked to different combinations of personality traits may further elucidate the factors that predispose individuals for leader or follower roles. Identifying such predispositions could lead to applied benefits in music pedagogy by allowing techniques for developing ensemble performance skills to be tailored to individuals (Keller 2013).

Implications for neurology and human–machine interaction stem from the possibility of using ADAM to drive robots or virtual agents that function as synchronization partners. Research and clinical practice in neurology has demonstrated the effectiveness of music-based interventions in the rehabilitation of motor dysfunctions associated with conditions including stroke and Parkinson's disease (e.g., Hove et al. 2012; Thaut et al. 2015). There are, however, marked individual differences in responsiveness to such interventions, for example, in the use of rhythmic auditory stimulation to improve gait in patients with Parkinson's disease (Dalla Bella et al. 2017). Using ADAM to drive the auditory stimulation sequences may provide an avenue for mitigating such individual differences. Indeed,

a related study on Parkinsonian gait found that using an adaptive auditory-pacing sequence coupled to patients' footfalls improved stability and reinstated healthy gait dynamics over-and-above conventional (non-adaptive) rhythmic auditory stimulation (Hove et al. 2012). Implementing the full complement of ADAM's three-module architecture may lead to further improvement. Moreover, such benefits may extend beyond clinical contexts and apply more generally in the domain of real-time human–machine interaction. For instance, preliminary work has revealed that implementing ADAM's adaptation and anticipation modules improves the fluency of human–robot teaming (Iqbal et al. 2016).

Finally, a theoretical point can be made regarding the potential hybridization of ADAM, a linear event-based model, with nonlinear dynamical models of sensorimotor synchronization (e.g., Dumas et al. 2014; Large et al. 2015; Tognoli and Kelso 2014). While the event-based approach adopted by ADAM seems appropriate for dealing with intentional actions, such as producing a series of discrete musical tones, the continuous body movements involved in such actions are likely best dealt with by the nonlinear dynamical approach. Therefore, as proposed in our previous work (MacRitchie et al. 2017; van der Steen and Keller 2013), we believe that it would be fruitful in future research to combine these classes of models using a hybrid architecture in which discrete events in ADAM provide a scaffold of 'anchor points' (Fink et al. 2000; Miyata et al. 2018) upon which the dynamics of continuous movements are hung.

6.4 Conclusions

The present study illustrates the behavior of the adaptive and anticipatory mechanisms employed by ADAM across different tempo conditions (steady tempo, tempo change) and interactive scenarios (single-agent, dual-agent) that are typically observed in tasks that require precise, yet flexible, sensorimotor synchronization (i.e., ensemble musical performance). By examining the behavior of the model parameters under single- and dual-agent conditions, the results enhance our understanding of how reactive error correction and predictive processes interact with the degree to which the agents possessed a shared representation of the temporal patterns entailed in the joint performance. The simulation framework outlined here promises to be a useful computational approach to complement laboratory and naturalistic studies to reveal the latent sensorimotor and cognitive mechanisms that give rise to different interpersonal coordination strategies that are negotiated by interacting agents.

Acknowledgements This work is supported by ARC Future Fellowship Grant FT140101162.

References

- Bavassi ML, Tagliazucchi E, Laje R (2013) Small perturbations in a finger-tapping task reveal inherent nonlinearities of the underlying error correction mechanism. *Hum Mov Sci* 32(1):21–47. <https://doi.org/10.1016/j.humov.2012.06.002>
- Blakemore S-J, Frith C (2005) The role of motor contagion in the prediction of action. *Neuropsychologia* 43(2):260–267. <https://doi.org/10.1016/j.neuropsychologia.2004.11.012>
- Colley ID, Keller P, Halpern AR (2017) Working memory and auditory imagery predict sensorimotor synchronization with expressively timed music. *Q J Exp Psychol*. <https://doi.org/10.1080/17470218.2017.1366531>
- Dalla Bella S, Benoit C-E, Farrugia N, Keller PE, Obrig H, Mainka S, Kotz SA (2017) Gait improvement via rhythmic stimulation in Parkinson's disease is linked to rhythmic skills. *Sci Rep*. <https://doi.org/10.1038/srep42005>
- Dumas G, de Guzman GC, Tognoli E, Kelso JAS (2014) The human dynamic clamp as a paradigm for social interaction. *Proc Natl Acad Sci* 111(35):E3726–E3734. <https://doi.org/10.1073/pnas.1407486111>
- Edwards AM, Guy JH, Hettinga FJ (2016) Oxford and Cambridge boat race: performance, pacing and tactics between 1890 and 2014. *Sports Med* 46(10):1553–1562. <https://doi.org/10.1007/s40279-016-0524-y>
- Fairhurst MT, Janata P, Keller PE (2013) Being and feeling in sync with an adaptive virtual partner: brain mechanisms underlying dynamic cooperativity. *Cereb Cortex* 23(11):2592–2600. <https://doi.org/10.1093/cercor/bhs243>
- Fairhurst MT, Janata P, Keller PE (2014) Leading the follower: an fMRI investigation of dynamic cooperativity and leader–follower strategies in synchronization with an adaptive virtual partner. *NeuroImage* 84:688–697. <https://doi.org/10.1016/j.neuroimage.2013.09.027>
- Fink PW, Foo P, Jirsa VK, Kelso JAS (2000) Local and global stabilization of coordination by sensory information. *Exp Brain Res* 134(1):9–20. <https://doi.org/10.1007/s002210000439>
- Gabriellsson A (2003) Music performance research at the millennium. *Psychol Music* 31(3):221–272. <https://doi.org/10.1177/03057356030313002>
- Gambi C, Pickering MJ (2011) A cognitive architecture for the coordination of utterances. *Front Psychol*. <https://doi.org/10.3389/fpsyg.2011.00275>
- Hary D, Moore GP (1987) On the performance and stability of human metronome-synchronization strategies. *Br J Math Stat Psychol* 40:109–124
- Hove MJ, Suzuki K, Uchitomi H, Orimo S, Miyake Y (2012) Interactive rhythmic auditory stimulation reinstates natural 1/f timing in gait of Parkinson's patients. *PLoS ONE* 7(3):e32600. <https://doi.org/10.1371/journal.pone.0032600>
- Iqbal T, Rack S, Riek LD (2016) Movement coordination in human-robot teams: a dynamical systems approach. *IEEE Trans Rob* 32(4):909–919. <https://doi.org/10.1109/TRO.2016.2570240>
- Jacoby N, Repp BH (2012) A general linear framework for the comparison and evaluation of models of sensorimotor synchronization. *Biol Cybern* 106(3):135–154. <https://doi.org/10.1007/s00422-012-0482-x>
- Jacoby N, Tishby N, Repp BH, Ahissar M, Keller PE (2015) Parameter estimation of linear sensorimotor synchronization models: phase correction, period correction, and ensemble synchronization. *Timing Time Percept* 3(1–2):52–87. <https://doi.org/10.1163/22134468-00002048>
- Keller PE (2008) Joint action in music performance. Enacting intersubjectivity: a cognitive and social perspective on the study of interactions. IOS Press, Amsterdam, pp 205–221
- Keller PE (2013). Musical ensemble performance: a theoretical framework and empirical findings on interpersonal coordination. In: Proceedings of the 4th international symposium on performance science (ISPS 2013), 28–31 August 2013, Vienna, pp 271–285
- Keller PE, Novembre G, Hove MJ (2014) Rhythm in joint action: psychological and neurophysiological mechanisms for real-time interpersonal coordination. *Philos Trans R Soc B Biol Sci* 369(1658):20130394. <https://doi.org/10.1098/rstb.2013.0394>
- Keller PE, Novembre G, Loehr J (2016) Musical ensemble performance: representing self, other, and joint action outcomes. In: Shared representations: sensorimotor foundations of social life, pp 280–310. Retrieved from <http://researchdirect.westernsydney.edu.au/islandora/object/uws%3A39000/>. Accessed 20 Oct 2017
- Kelso JAS, de Guzman GC, Reveley C, Tognoli E (2009) Virtual partner interaction (VPI): exploring novel behaviors via coordination dynamics. *PLoS ONE* 4(6):e5749. <https://doi.org/10.1371/journal.pone.0005749>
- Knoblich G, Jordan JS (2003) Action coordination in groups and individuals: learning anticipatory control. *J Exp Psychol Learn Mem Cogn* 29(5):1006–1016. <https://doi.org/10.1037/0278-7393.29.5.1006>
- Konvalinka I, Vuust P, Roepstorff A, Frith CD (2010) Follow you, follow me: continuous mutual prediction and adaptation in joint tapping. *Q J Ex Psychol* 63(11):2220–2230. <https://doi.org/10.1080/17470218.2010.497843>
- Large EW, Herrera JA, Velasco MJ (2015) Neural networks for beat perception in musical rhythm. *Front Syst Neurosci*. <https://doi.org/10.3389/fnsys.2015.00159>
- Loehr JD, Large EW, Palmer C (2011) Temporal coordination and adaptation to rate change in music performance. *J Exp Psychol Hum Percept Perform* 37(4):1292–1309. <https://doi.org/10.1037/a0023102>
- MacRitchie J, Herff SA, Procopio A, Keller PE (2017a) Negotiating between individual and joint goals in ensemble musical performance. *Q J Ex Psychol*. <https://doi.org/10.1080/17470218.2017.1339098>
- MacRitchie J, Varlet M, Keller PE (2017). Embodied expression through entrainment and co-representation in musical ensemble performance. In: The Routledge companion to embodied music interaction. Routledge, London. <https://doi.org/10.4324/9781315621364.ch16>
- Mates J (1994a) A model of synchronization of motor acts to a stimulus sequence. I. Timing and error corrections. *Biol Cybern* 70(5):463–473
- Mates J (1994b) A model of synchronization of motor acts to a stimulus sequence. II. Stability analysis, error estimation and simulations. *Biol Cybern* 70(5):475–484
- McAuley JD, Jones MR (2003) Modeling effects of rhythmic context on perceived duration: a comparison of interval and entrainment approaches to short-interval timing. *J Exp Psychol Hum Percept Perform* 29(6):1102–1125. <https://doi.org/10.1037/0096-1523.29.6.1102>
- Michon JA (1967) Timing in temporal tracking. Institute for Perception RVO-TNO, Soesterberg
- Mills PF, van der Steen MC, Schultz BG, Keller PE (2015) Individual differences in temporal anticipation and adaptation during sensorimotor synchronization. *Timing Time Percept*. <https://doi.org/10.1163/22134468-03002040>
- Miyata K, Varlet M, Miura A, Kudo K, Keller PE (2018) Interpersonal visual interaction induces local and global stabilisation of rhythmic coordination. *Neurosci Lett*. <https://doi.org/10.1016/j.neulet.2018.07.024>
- Néda Z, Ravasz E, Brechet Y, Vicsek T, Barabási A-L (2000) Self-organizing processes: the sound of many hands clapping. *Nature* 403(6772):849–850. <https://doi.org/10.1038/35002660>

- Novembre G, Ticini LF, Schütz-Bosbach S, Keller PE (2014) Motor simulation and the coordination of self and other in real-time joint action. *Soc Cogn Affect Neurosci* 9(8):1062–1068. <https://doi.org/10.1093/scan/nst086>
- Novembre G, Varlet M, Muawiyath S, Stevens CJ, Keller PE (2015) The E-music box: an empirical method for exploring the universal capacity for musical production and for social interaction through music. *R Soc Open Sci*. <https://doi.org/10.1098/rsos.150286>
- Novembre G, Sammler D, Keller PE (2016) Neural alpha oscillations index the balance between self-other integration and segregation in real-time joint action. *Neuropsychologia* 89:414–425. <https://doi.org/10.1016/j.neuropsychologia.2016.07.027>
- Nowicki L, Prinz W, Grosjean M, Repp BH, Keller PE (2013) Mutual adaptive timing in interpersonal action coordination. *Psychomusicol Music Mind Brain* 23(1):6–20. <https://doi.org/10.1037/a0032039>
- Pecenka N, Keller PE (2009) Auditory pitch imagery and its relationship to musical synchronization. *Ann N Y Acad Sci* 1169(1):282–286. <https://doi.org/10.1111/j.1749-6632.2009.04785.x>
- Pecenka N, Keller PE (2011) The role of temporal prediction abilities in interpersonal sensorimotor synchronization. *Exp Brain Res* 211(3–4):505–515. <https://doi.org/10.1007/s00221-011-2616-0>
- Pecenka N, Engel A, Keller PE (2013) Neural correlates of auditory temporal predictions during sensorimotor synchronization. *Front Hum Neurosci* 7:380. <https://doi.org/10.3389/fnhum.2013.00380>
- Phillips-Silver J, Aktipis CA, Bryant GA (2010) The ecology of entrainment: foundations of coordinated rhythmic movement. *Music Percept Interdiscip J* 28(1):3–14. <https://doi.org/10.1525/mp.2010.28.1.3>
- Pressing J (1999) The referential dynamics of cognition and action. *Psychol Rev* 106(4):714–747. <https://doi.org/10.1037/0033-295X.106.4.714>
- Ragert M, Schroeder T, Keller PE (2013) Knowing too little or too much: the effects of familiarity with a co-performer's part on interpersonal coordination in musical ensembles. *Front Psychol* 4:368. <https://doi.org/10.3389/fpsyg.2013.00368>
- Rankin SK, Large EW, Fink PW (2009) Fractal tempo fluctuation and pulse prediction. *Music Percept Interdiscip J* 26(5):401–413. <https://doi.org/10.1525/mp.2009.26.5.401>
- Repp BH (2002) The embodiment of musical structure: effects of musical context on sensorimotor synchronization with complex timing patterns. In: Prinz W, Hommel B (eds) *Common mechanisms in perception and action: attention and performance XIX*. Oxford University Press, Oxford, pp 245–265
- Repp BH (2005) Sensorimotor synchronization: a review of the tapping literature. *Psychon Bull Rev* 12(6):969–992. <https://doi.org/10.3758/BF03206433>
- Repp BH, Keller PE (2004) Adaptation to tempo changes in sensorimotor synchronization: effects of intention, attention, and awareness. *Q J Ex Psychol Section A* 57(3):499–521. <https://doi.org/10.1080/02724980343000369>
- Repp BH, Keller PE (2008) Sensorimotor synchronization with adaptively timed sequences. *Hum Mov Sci* 27(3):423–456. <https://doi.org/10.1016/j.humov.2008.02.016>
- Repp BH, Keller PE (2010) Self versus other in piano performance: detectability of timing perturbations depends on personal playing style. *Exp Brain Res* 202(1):101–110. <https://doi.org/10.1007/s00221-009-2115-8>
- Repp BH, Su Y-H (2013) Sensorimotor synchronization: a review of recent research (2006–2012). *Psychon Bull Rev* 20(3):403–452. <https://doi.org/10.3758/s13423-012-0371-2>
- Repp BH, Keller PE, Jacoby N (2012) Quantifying phase correction in sensorimotor synchronization: empirical comparison of three paradigms. *Acta Physiol (Oxf)* 139(2):281–290. <https://doi.org/10.1016/j.actpsy.2011.11.002>
- Sänger J, Lindenberger U, Müller V (2011) Interactive brains, social minds. *Commun Integr Biol* 4(6):655–663. <https://doi.org/10.4161/cib.17934>
- Schiavio A, Høffding S (2015) Playing together without communicating? a pre-reflective and enactive account of joint musical performance. *Music Sci* 19(4):366–388. <https://doi.org/10.1177/1029864915593333>
- Schulze H-H, Cordes A, Vorberg D (2005) Keeping synchrony while tempo changes: accelerando and ritardando. *Music Percept Interdiscip J* 22(3):461–477. <https://doi.org/10.1525/mp.2005.22.3.461>
- Sebanz N, Knoblich G (2009) Prediction in joint action: what, when, and where. *Top Cogn Sci* 1(2):353–367. <https://doi.org/10.1111/j.1756-8765.2009.01024.x>
- Skewes JC, Skewes L, Michael J, Konvalinka I (2015) Synchronised and complementary coordination mechanisms in an asymmetric joint aiming task. *Exp Brain Res* 233(2):551–565. <https://doi.org/10.1007/s00221-014-4135-2>
- Thaut MH, McIntosh GC, Hoemberg V (2015) Neurobiological foundations of neurologic music therapy: rhythmic entrainment and the motor system. *Front Psychol* 5:1. <https://doi.org/10.3389/fpsyg.2014.01185>
- Tognoli E, Kelso JAS (2014) The metastable brain. *Neuron* 81(1):35–48. <https://doi.org/10.1016/j.neuron.2013.12.022>
- Torre K, Balasubramaniam R (2009) Two different processes for sensorimotor synchronization in continuous and discontinuous rhythmic movements. *Exp Brain Res* 199(2):157–166. <https://doi.org/10.1007/s00221-009-1991-2>
- van der Steen MC, Keller PE (2013) The adaptation and anticipation model (ADAM) of sensorimotor synchronization. *Front Hum Neurosci* 7:253. <https://doi.org/10.3389/fnhum.2013.00253>
- van der Steen MC, Jacoby N, Fairhurst MT, Keller PE (2015a) Sensorimotor synchronization with tempo-changing auditory sequences: modeling temporal adaptation and anticipation. *Brain Res* 1626:66–87. <https://doi.org/10.1016/j.brainres.2015.01.053>
- van der Steen MC, Schwartze M, Kotz SA, Keller PE (2015b) Modeling effects of cerebellar and basal ganglia lesions on adaptation and anticipation during sensorimotor synchronization. *Ann N Y Acad Sci* 1337(1):101–110. <https://doi.org/10.1111/nyas.12628>
- Vorberg D (2005, July) Synchronization in duet performance: testing the two-person phase error correction model. Presented at the 10th rhythm perception and production workshop, Alden Biesen
- Vorberg D, Hambuch R (1978) On the temporal control of rhythmic performance. In: Requin J (ed) *Attention and performance*, vol VII. Erlbaum, Hillsdale NJ, pp 535–555
- Vorberg D, Schulze H-H (2002) Linear phase-correction in synchronization: predictions, parameter estimation, and simulations. *J Math Psychol* 46(1):56–87. <https://doi.org/10.1006/jmps.2001.1375>
- Vorberg D, Wing A (1996) Modeling variability and dependence in timing. In: Heuer H, Keele S (eds) *Handbook of perception and action*. Academic, London, pp 181–262
- Wing AM (1993) The uncertain motor system: perspectives on the variability of movement. In: Meyer DE, Kornblum S (eds) *Attention and performance XIV: synergies in experimental psychology, artificial intelligence, and cognitive neuroscience*. The MIT Press, Cambridge, pp 709–744
- Wing AM, Kristofferson AB (1973) Response delays and the timing of discrete motor responses. *Percept Psychophys* 14(1):5–12. <https://doi.org/10.3758/BF03198607>
- Wing AM, Endo S, Bradbury A, Vorberg D (2014) Optimal feedback correction in string quartet synchronization. *J R Soc Interface* 11(93):20131125. <https://doi.org/10.1098/rsif.2013.1125>

- Wolpert DM, Kawato M (1998) Multiple paired forward and inverse models for motor control. *Neural Netw* 11(7):1317–1329. [https://doi.org/10.1016/S0893-6080\(98\)00066-5](https://doi.org/10.1016/S0893-6080(98)00066-5)
- Wolpert DM, Doya K, Kawato M (2003) A unifying computational framework for motor control and social interaction. *Philos Trans R Soc B Biol Sci* 358(1431):593–602. <https://doi.org/10.1098/rstb.2002.1238>

Publisher's Note Springer Nature remains neutral with regard to jurisdictional claims in published maps and institutional affiliations.